Fuel 346 (2023) 128233

Contents lists available at ScienceDirect

Fuel

journal homepage: www.elsevier.com/locate/fuel

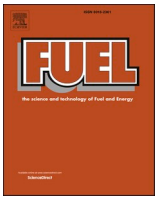

Investigation of gasification reactivity and properties of biocarbon at high temperature in a mixture of CO/CO_2

Liang Wang [a,*], Øyvind Skreiberg [a], Nicholas Smith-Hanssen [b], Sethulakshmy Jayakumari [b], Stein Rørvik [b], Gøril Jahrsengene [b], Scott Turn [c]

[a] SINTEF Energy Research, P.O. Box 4761 Torgarden, Trondheim NO-7465, Norway
[b] SINTEF Industry, Richard Birkelands vei 3, Trondheim NO-7034, Norway
[c] Hawaii Natural Energy Institute, School of Ocean and Earth Science and Technology, University of Hawaii at Manoa, Honolulu, HI 96822, United States

A B S T R A C T

Understanding the conversion behaviors of biocarbon under conditions relevant to industrial conditions is important to ensure proper and efficient utilization of the biocarbon for a dedicated metallurgical process. The present work studied the reactivity of biocarbon by using a Macro-TGA at 1100 °C in a gas mixture of CO_2 and CO to simulate the conditions in an industrial closed submerged arc manganese alloy furnace. The conversion residues from the Macro-TGA tests were collected for detailed characterization through a combination of different analytical techniques. Results showed that biocarbons produced under various conditions have different reactivities under the studied conditions. The biocarbon produced in an atmospheric fixed bed reactor with continuous purging of N_2 has the highest reactivity. Its fixed carbon loss started as the gas atmosphere shifted from the inert Ar to a mixture of CO and CO_2 at 1100 °C. And only 450 s was needed to reach a desired fixed-carbon loss of 20%. The high reactivity of the biocarbon is mainly related to its porous structure and high content of catalytic inorganic elements, which favor gasification reactions of the carbon matrix towards the surrounding gas atmosphere and consumption of carbon consequently. In contrast, biocarbon produced under constrained conditions and from wood pellets and steam exploded pellets have more compact appearance and dense structures. Significant fixed carbon loss for these biocarbons started 80–200 s later than that of the biocarbon produced at atmospheric conditions with purging of N_2. Additionally, it took longer time, 557–1167 s, for these biocarbons to realize the desired fixed-carbon loss. SEM-EDX analyses results revealed clear accumulation and aggregation of inorganic elements, mainly Ca, on the external surface of the residues from gasification of biocarbon produced in the fixed bed reactor with purging of N_2. It indicates more intensive migration and transformation of inorganic elements during gasification at this condition. This resulted in formation of a carbon matrix with more porous structure and active sites on the carbon surface, promoting the Boudouard reaction and conversion of carbon.

1. Introduction

The anthropogenic emissions of greenhouse gases have reached a historically high level and is considered as the main reason for global warming. With consideration of increasing demands for energy, power and materials, it can be expected that the greenhouse gas emissions from human activities will continue to increase, leading to even more severe changes in the global climate [39]. Metal production is one of the most energy and carbon-intensive industrial processes. Fossil carbon is used as a source of carbon, and in some metallurgical processes, energy, for metal production, and is responsible for a large amount of direct CO_2 emissions annually. To decrease the emissions, several measures have been considered, developed and tested, including implementing of breakthrough technologies, replacement of fossil carbon with carbon from renewable sources (i.e., biocarbon), capture and storage of CO_2 and increased energy and material utilization and recovery efficiency [41,42,54]. In comparison to other measures, usage of biocarbon for metal production has been considered as a promising and straightforward way to reduce dependency on fossil carbon and emissions of greenhouse gases in a short time. The usage of biocarbon in metallurgical applications can reduce CO_2 emissions from the metal production processes to the environment and dependence on fossil carbon [42]. In addition, biocarbon can be produced from different bio-based materials derived from waste streams. Therefore, production and utilization of biocarbon can also help to realize management and conversion of waste to valuable products, which leads to more social and economic benefits [53].

The biocarbon for metal production is normally produced through carbonization, or slow pyrolysis, of biomass materials. The yield and properties of the biocarbon heavily depend on the source of feedstock and production conditions [44]. Currently, woody biomasses are used as main raw feedstocks for biocarbon production, due to their high availability and rather consistent properties [41,42]. Properties of the biocarbon produced from woody biomass are normally superior to those

* Corresponding author.

https://doi.org/10.1016/j.fuel.2023.128233
Received 13 January 2023; Received in revised form 11 March 2023; Accepted 24 March 2023
Available online 13 April 2023

produced from other biomass materials, including relatively low ash content, high bulk and energy density and better mechanical properties [49]. Production conditions can also significantly affect pyrolysis behaviors, mass and carbon conversion efficiency and characteristics of biocarbon. Mass yield and fixed-carbon content of the biocarbon provided by conventional production processes are generally low, partly due to limited control of the carbonization process. This increases feedstock consumption, logistics and reduces biocarbon value chain profitability. Studies have been conducted to investigate the possibility to manipulate process conditions to improve the yield of solid biocarbon and the fixed carbon content of it [22,21,26,45,50]. The results showed that improvement of biocarbon and fixed-carbon yield can be realized by extending the residence time of pyrolysis vapors, using large particles, increasing carbonization pressure etc. This promotes secondary reactions that enhance tar cracking and recondensation onto the charring particles, thereby increasing yields of biocarbon and fixed carbon [12,38,45,50]. As used for metallurgical applications, quality of the biocarbon is closely related to physio-chemical properties of the biocarbon. However, properties of the biocarbon can be significantly different, when produced from different biomass materials and under different conditions. Therefore, detailed analysis and assessment of biocarbon properties are primary steps to ensure proper and efficient utilization of biocarbon in a specific metallurgical process. The analyses results are also important to predict behaviors of the biocarbons when they act as reductant and to assess effects of them on metal production processes.

In the production of metal (e.g., ferromanganese), the carbon reductant enters from the top of the smelting furnace. A schematic drawing of such a furnace showing also possible conversion reactions of the carbon reductant in the furnace can be found in Lindstad's work [24]. The solid carbon reductant flows downwards and passes through a pre-reduction zone with elevated temperatures and mixtures of gases (i.e., CO and CO_2) and volatilized species (e.g., K, which acts as a catalyst), before it reaches the slag zone in the furnace bottom to react with metal ores [16,17,24]. During this process, the carbon reductant normally undergoes reactions during the processes of drying, devolatilization, calcination and gasification [15]. Some of the reactions can overlap and the extents of the them are related to local conditions and progressing property changes of reductant particles [24]. The high reactivity of the carbon reductant towards surrounding gases are undesirable in e.g., manganese alloy production, since it causes considerable consumption of carbon and heat in the upper part of the furnace, which often is related to significant CO_2 emissions as well [17]. In addition to the chemical reactions, during the movement, the carbon reductant also undergoes mechanical actions such as crushing and extruding, resulting in fragmentation of the original reductant particles and formation of fines. The fines originating from the carbon reductant in the lower part of the furnace tend to flow further down and accumulate in the slag zone at the bottom of the furnace or travel upward in the furnace [18]. The fines escaping from the furnace is related to loss of carbon that thus does not involve in chemical reactions with metal ores. In addition, formation of a large amount of fines can arise risk of explosion and cause downstream operational problems such as clogging of pipes [33]. Moreover, the carbon reductant particles with small sizes react in a short time and cannot reach the slag zone, contributing to loss of carbon reductant. All the chemical reactions and mechanical actions cause degradation and consumption of the carbon reductant in the pre-reduction zone. Therefore, it is necessary to investigate and assess conversion behaviors and reactivity of biocarbon under industrial relevant conditions.

Gasification leads to degradation and change of physio-chemical properties of the carbon reductant as it descends through the smelting furnace. Gasification of industrial coke has been investigated under CO_2 atmosphere because it is more prevalent in the metal production processes[6,10,31]. Gasification reactivity of the carbon reductant is one of the most important parameters to assess and evaluate regarding performance of it in the metallurgical processes[56]. The ASTM Standard for measuring CO_2 reactivity of carbon reductant for metal production is conducted in a 100% CO_2 atmosphere at 1100 °C. Studies by using thermogravimetric analysis (TGA) systems or setups with similar principles have been conducted to investigate conversion behaviors of the coke and correlate reactivity of the coke with its critical properties [10,14,31]. However, as approaching the lowest part of the pre-reduction zone, the temperature is about 1000–1400 °C with a mixture of CO_2 and CO around the carbon reductant. Better understanding of conversion behaviors of the biocarbon under such complicated conditions are critically important. Therefore, reactivity of carbon reductants, mainly ordinary metallurgical coke, has been tested in an atmosphere of 75% CO and 25% CO_2 or 50% CO and 50% CO_2, at 800–1100 °C by using a thermobalance apparatus. The results showed that the coke has low reactivity under studied conditions up to 1000 °C. As the reaction temperature is over 1000 °C, there was evident increase of reactivity with increase of partial pressure of CO_2 [24,56]. However, studies of reactivity of biocarbons under industrial relevant conditions, i.e., high temperature and in a mixture of CO and CO_2, are seldom. Kaffash et al. studied reactivity of industrial biocarbon in a gas mixture of 50% CO_2 and 50% CO and a temperature of 1070 °C in a thermogravimetric analyser (TGA). The main focus of the work was to study the effect of densification of biocarbon by methane deposition on its reactivity under studied conditions. One metallurgical coke was also studied for comparison purpose. The results showed that the studied biocarbons have evidently higher reactivities than that of metallurgical coke. The difference is mainly due to that the biocarbon, compared to the coke, has high surface area/porosity and content of catalytic ash elements and more reactive carbon structure [16,17]. Densification treatment by depositing carbon from methane decreased reactivity of the biocarbon. However, as industrial biocarbons were used in these studies, no information was reported regarding source of raw biomass and process parameters for producing them. It was therefore not possible to correlate biocarbon production conditions and their reactivity. Therefore, the results are less useful for designing processes to produce biocarbon with desired properties for metal production processes. In addition, past research focused mainly on studying gasification behaviours of biocarbon, while characteristics of the biocarbon after gasification tests were rarely provided. However, the properties of the biocarbon after passing through the pre-reduction zone can be significantly different to those of the initial biocarbon fed into the furnace. The partially reacted biocarbon is the final carbon mass that will meet and react with metal ores in the slag zone. This part of the biocarbon will play a decisive role to determine metal reduction efficiency and affect quality of the metal products. Better understanding and detailed characterization of the gasified biocarbon are crucial for improving performance of it as reductant for metal production.

In this study, biocarbons were produced under different conditions and from different feedstocks with different physio-chemical properties. Gasification reactivity of the produced biocarbon were studied by using a macro thermogravimetric analyser (Macro-TGA) at 1100 °C in a gas mixture of CO and CO_2. Critical properties of raw biocarbon and reacted biocarbon after gasification tests were investigated including element composition, content of inorganic elements, microstructure and microchemistry and mechanical strength. The main objectives of the current work are to (1) study gasification behaviours of biocarbon under industrial relevant conditions, which were produced under different process parameters, and (2) conduct detailed characterization of the conversion residues.

2. Experimental

2.1. Biomass feedstock

In this work, birch wood chips, spruce wood pellets and steam-exploded pellets were used for biocarbon production. A birch tree was harvested in southern Norway and shredded into chips with sizes of 2–4

cm. The birch wood chips were then dried in a drying oven for 12 h before the carbonization experiment. As used for metallurgical applications, biocarbon with high carbon content and low reactivity is desired. Pelletization of woody biomass materials is an efficient measure to improve quality of the woody biomass, for enhancing homogeneity and energy and bulk density. Steam explosion combined with pelletization is another efficient way that can further upgrade woody biomass into a high-quality solid commodity [52]. In addition, biomass pellets, compared to wood chips, with rather uniform sizes and properties are also easier for handling, transportation and storage. It is expected that the biocarbon produced from wood pellets and steam-exploded pellets preserve a dense structure and low porosity, and can be sources of carbon for metal production processes. Therefore, for broadening bio-based sources for biocarbon production, wood pellets (white pellets) and steam-exploded pellets were studied in the current work. Both pellets have a diameter of 8 mm with a length of about 65 mm.

2.2. Biocarbon production

The biocarbon samples for the Macro-TGA gasification reactivity tests were produced under different conditions. The first group of biocarbon samples was produced by using an apparatus comprising a vertical tubular fixed-bed reactor, a condenser and a gas monitoring system. For one biocarbon production experiment, the pre-dried wood chips or pellets were first placed into the vertical tubular reactor, about 700g, respectively. After loaded with the sample, the tubular reactor was sealed and placed inside an electrical furnace, which was then connected to the gas supply and monitoring system and the condenser. The electrical furnace has three heating zones. The temperature in the reactor was controlled and monitored by three thermocouples along the length of the electrical furnace. Before start of one experiment, N_2 gas flows into the tubular reactor from the bottom with a flow rate of 2 L min^{-1} as purge gas to flush away residual air and generate an inert atmosphere, avoiding possible oxidization and ignition of the sample during the heating up stage. After purging with the nitrogen at room temperature for 1 h, the sample was heated up to 500 °C at a heating rate of 10 °C min^{-1}, and was kept at this temperature for 1 h. During running of one experiment, volatiles and tarry vapors that are generated due to decomposition of the biomass feedstock, leave the reactor and reach the condenser. The condensable fractions of volatiles and tarry vapors were collected by the condenser and the incondensable fraction further flow through filters and its composition was monitored continuously by a micro gas chromatograph (Varian Cp-4900), equipped with two injectors connected to individual columns.

It has been widely reported that the yield and properties of products from carbonization of biomass are considerably affected by process conditions and characteristics of biomass feedstock [30,29,28,50]. The carbonization conditions, including the highest heating temperature, heating rate, purge gas flow rate and pressure, are critical to determine distribution and properties of the products from the carbonization of biomass. One of the main objectives of the biocarbon production experiments was to study the effect of pyrolysis conditions on yields and properties of the products, focusing on enhancing the yield of fixed carbon. Therefore, the biocarbons were produced using the tubular reactor with two different atmospheres, with and without using of nitrogen as purge gas. For the experiment performed under a nitrogen atmosphere, the purge gas flow rate was set to 2 L min^{-1}, which generates an inert atmosphere during one pyrolysis experiment. For the experiments conducted without purging of N_2, it enables extending the residence time of the volatiles and tarry vapours and consequently promotes secondary reactions of them. It improves yield and alters properties of the produced solid biocarbon. Different from the experiments conducted with purging of N_2, the pyrolysis of one sample will take place in presence of gases (i.e., CO_2, CO, CH_4) that are generated due to decomposition of the sample at elevated temperatures. For further prolonging residence time of the volatiles in the reactor, a lid was put on the top of the biomass sample bed. The distance between the rim of the lid and the internal tubular reactor surface was about 2 mm. In addition to linear heating experiments, one staged heating experiment was carried out for comparison purpose. After initial purging with N_2 for 1 h, the birch wood chips were heated up to 350 °C with a linear heating rate of 10 K/min and kept at this temperature for 1 h. Then the chips were further heated up to 500 °C with the same heating rate. For all experiments conducted with and without purge gas, after the sample was heated up to 500 °C and with sufficient holding time, the electricity to the furnace was shut off and the reactor was cooled down with continuous purging of nitrogen gas. As the reactor was cooled down to room temperature, the solid biocarbon and liquid condensates were collected and weighed, and were then stored for further characterization and testing purpose.

The second group of biocarbon samples were produced under pressure by using the flash carbonization reactor at the University of Hawaii. The reactor and normal operation procedures were described in our previous work, and only a brief introduction is given here [44]. For one flash carbonization experiment, pre-dried birch wood chips were weighed and placed in a canister. The canister was then loaded into a vessel that was sealed and pressurized with air to a set value. After the pressure in the reactor reaches the desired value, the loaded birch wood chips were ignited by an electrical heating coil at the bottom of the reactor [50]. The ignitor was turned off after 6 min ignition time. Following the ignition, compressed air was delivered from the top of the reactor and flowed downward through the feedstock bed [45]. At the same time, ignition induced flash fire of the feedstock and the flame front moved upward and against the flow of air, resulting in the conversion of the feedstock into biocarbon. The pressure in the reactor was continuously monitored and maintained at a preset value by a pressure-reduction valve located downstream of the reactor. After sufficient air was delivered to carbonize the wood, the airflow was halted and the reactor cooled down. In the present work, the birch wood chips were carbonized at pressures of about 7.9 and 21.7 bar. More details about the pressurized carbonization experiments can be found in our previous work [45]. In total, seven biocarbon samples were produced for the Macro-TGA gasification reactivity study, including birch wood biocarbon produced at 500 °C with purging of N_2 (BC-500-P), birch wood biocarbon produced at 500 °C without purging of N_2 and with a lid (BW 500-NPL), birch wood biocarbon produced via staged carbonization without purging of N_2 (BW 350–500-NP), wood pellets carbonized at 500 °C without purging of N_2 (WP 500-NP), steam exploded pellets carbonized at 500 °C without purging of N_2 (SP 500-NP), birch wood biocarbon produced under pressure of 7.9 bar (BW-7.9 bar), and birch wood biocarbon produced under pressure of 21.7 bar (BW-21.7 bar).

2.3. Macro-TGA reactivity test

The reactivity tests were conducted by using a Macro-TGA with controlled temperature and gas atmosphere, as is schematically shown in Fig. 1 The main components of the Macro-TGA are an electric cylindrical furnace, a Mettler Toledo PB 1502 balance (with an accuracy of 0.1 g), and a crucible. The temperature of the furnace was controlled by a thermocouple connected to a Eurotherm 2408 controller that is controlled and monitored continuously. For one gasification experiment, 20 g of biocarbon was first loaded in the crucible on a ceramic perforable plate. Then the crucible was further hooked up with the balance. After samples loading, the furnace is hoisted and purged with argon for half an hour to flush away residual air. Then the data logger is started and the furnace is heated up from room temperature to 1100 °C. The sample was held at this temperature for half an hour. Then a gas mixture of 50% CO_2 and 50% CO was fed with a flow rate of 4 Nl/min into the furnace. The change of sample weight, the temperature in middle of the sample bed and the off-gas composition were continuously measured and logged. During the heating up from room temperature to 1100 °C with a heating rate of 10 K/min and a further half-hour holding

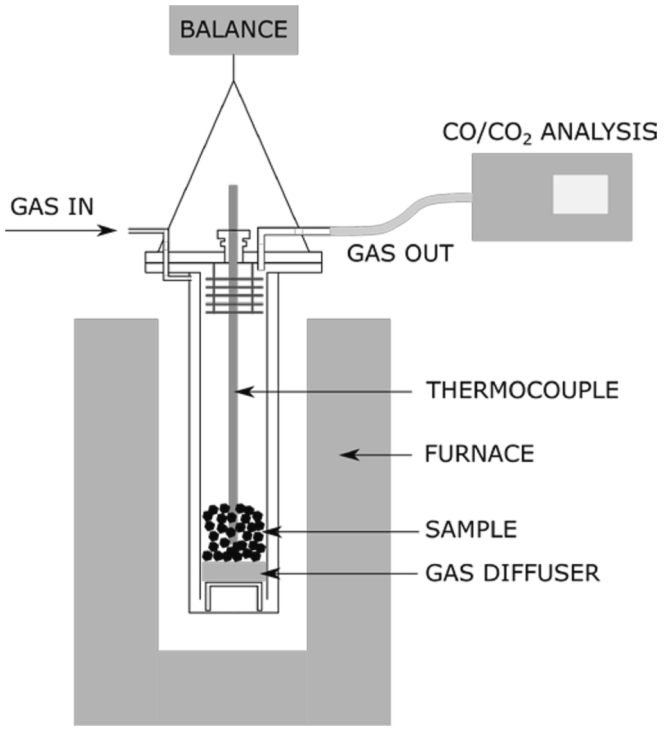

Fig. 1. Macro-TGA setup for studying gasifcation reactivity of biocarbon [17].

time at this temperature, devolatilization of the biocarbon takes place and the devolatilized biocarbon mainly contains carbon and small amounts of inorganic elements. The weight change during the following gasification of one sample is mainly due to loss of fixed carbon. In addition, it is necessary to collect partially gasified biocarbon for further characterization and comparison purposes. Therefore, as a weight loss corresponding to 20% of the fixed carbon was reached, the experiment was stopped with turning off the power to the furnace. The CO/CO_2 mixture was then replaced with argon and the furnace cooled down gradually. As the crucible temperature reached 50 °C, the logging was stopped, the argon flow was turned off, and the remaining biocarbon was collected and weighed. The gasification temperature and atmosphere were selected with considering the relevance for industrial-scale metal production processes. For example, in a smelting furnace to produce manganese alloy, the charge, including the carbon reductant, fed from the top of the furnace will flow downward through the pre-reduction zone before meeting the metal ore. In the end of the pre-reduction zone, the charge temperature is often typically around 1250 °C while the gas flowing upwards typically has a temperature of around 1400 °C. The Boudouard reaction of the carbon reductant takes place with presence of both CO_2 and CO in this gas surrounding the solid carbon reductant. The Macro-TGA setup has been used for studying reactivity of carboneous reductant in previous studies [16,17,24].

2.4. Characterization of raw and reacted biocarbon

2.4.1. General properties of biomass and produced biocarbon

Proximate analysis of pre-dried biomass and produced biocarbon samples was conducted in accordance with ASTM standard D1762-84. The dried sample, after the moisture content was measured, was loaded in a covered crucible and heated up to 950 °C for 11 min to determine the volatiles content and thereafter for determining the ash content, to 750 °C for 8 h (uncovered crucible). The sample weight differences before and after heating was determined as volatile matter content and ash content. The difference between the weight of the original sample and the sum of volatile matter content and ash content corresponds to the fixed carbon content. For each sample, triplicate analyses were conducted. Average values of the analyses are presented in Table 1.

2.4.2. Element analysis

The elemental composition of pre-dried biomass samples, biocarbon produced from them and residues after the Macro-TGA gasification experiments were analyzed by employing an elemental analyzer (Eurovector EA 3000 CHNS-O Elemental Analyser). Oxygen content of one sample was calculated by difference.

2.4.3. Inorganic element analysis

Contents of inorganic elements in the pre-dried biomasses, produced biocarbon and residual biocarbon after Macro-TGA gasification tests were measured using an inductively coupled plasma-atomic emission spectrometer (ICP-AES). One sample was dissolved in a mixture of acids (HNO_3, HF and H_3BO_3) and went through a pressurized multi-step digestion process, according to procedures described in the standard CEN/TS 15290:2006. The digested solution was then analyzed by the ICP-AES for elemental detection. Triplicate analyses were conducted for each sample and average values are presented.

2.4.4. SEM-EDX analysis of biocarbon

The microstructure and morphology of the biocarbons produced under different conditions and after the Macro-TGA gasification reactions were examined by using a scanning electron microscope (Zeiss Ultra 55 Limited Edition). One biocarbon grain was placed on a sample holder and placed into the SEM chamber, which was scanned with increasing magnifications to reveal details regarding surface morphology and microstructure of the studied biocarbon samples. The

Table 1
Characteristics of birch wood, wood pellet and steam-exploded pellets for biocarbon production.

		Birch wood (BW)	Wood pellet (WP)	Steam exploded pellet (SP)
Volatile matter	wt%, d.b.	84.43	86.66	82.14
Ash content	wt%, d.b.	0.78	0.51	0.34
Fixed-C*	wt%, d.b.	14.79	12.83	17.52
C	wt%, daf	45.9	47.08	51.92
H	wt%, daf	6.01	6.12	6.15
N	wt%, daf	0.13	0.08	0.10
S	wt%, daf	0.02	0.02	0.01
O*	wt%, daf	47.91	46.66	41.82
K	mg/kg, d.b.	278.8	530.0	480.0
Ca	mg/kg, d.b.	684.3	960.0	970.0
P	mg/kg, d.b.	65.8	70.0	60.0
Si	mg/kg, d.b.	20.3	57.0	65.3
Na	mg/kg, d.b.	14	10.1	11.1
S	mg/kg, d.b.	29.5	20.0	15.0
Mg	mg/kg, d.b.	221.0	154.0	146.0
Al	mg/kg, d.b.	20.2	4.0	4.0
Fe	mg/kg, d.b.	15.7	50.0	39.0
Mn	mg/kg, d.b.	83.8	98.0	42.0
Cu	mg/kg, d.b.	0.7	0.6	0.6
Zn	mg/kg, d.b.	25.4	4.4	5.4

d.b.: dry basis; daf: dry ash free basis; *: calculated by difference.

SEM is equipped with an energy-dispersive X-ray spectroscope (EDX). The combination of SEM and EDX enables to study the microchemistry of the biocarbon after the Macro-TGA gasification reaction. This is important to reveal the transportation/migration of inorganic elements in the biocarbon and their roles during the biocarbon gasification process.

2.4.5. μCT analysis of biocarbon

The microstructure of unreacted and gasified biocarbon was also analyzed, by a Nikon XT H 225 ST instrument (cone beam volume CT). For a scanning, a tungsten reflection target was used, with an acceleration voltage of 150 kV and a current of 150 μA. The X-rays were not filtered. The imaging was done with an integration time of 708 ms, signal amplification of 18 dB, with 6283 projections per 360° rotation. The detector panel in the instrument is a Perkin Elmer 1620 AN CS model with 2000x2000 pixels sized 200x200 μm; total panel size 40x40 cm^2. The distance from the source to the sample varied from 32.08 mm to 126.08 mm, resulting in a voxel size varying from 5.7 μm to 22.4 μm. The images were exported as 16-bit TIFF and processed in the public domain software Image [37] and using scripts developed at SINTEF. More details about image processing can be found in work reported by Rorvik et al. [34]. μCT analyses of biocarbon were conducted on the biocarbon samples before and after Macro-TGA gasification experiments. For a better comparison, several pieces of unreacted biocarbon were first scanned by the μCT. These biocarbon pieces were then placed in the crucible with known locations. After the Macro-TGA gasification reaction, they were collected and scanned with the μCT again. It enabled to scan and compare the microstructure of the exact same biocarbon pieces before and after gasification experiments.

2.4.6. Mechanical properties of carbonized pellets before and after Macro-TGA study

Mechanical properties are among the most important properties of biocarbon as used for metallurgical applications [42]. In the current work, the mechanical strength measurements were conducted for pre-dried biomass pellets, biomass pellets carbonized at 500 °C and the carbonized pellets after the Macro-TGA gasification at 1100 °C. The mechanical strength of pellets was tested by a pellet hardness tester (Amandus Kahl, Germany). One pellet was loaded in the hardness tester and compressed perpendicular to the cylindrical axis direction until identification of failure of the sample. The tensile compressive strength of one pellet was measured in kilograms by an equivalence between the elastic compression of a spring that moves a piston against the pellet side and the force equivalent mass [48]. As the studied pellet fractured into two parts along the loading axis, the applied force was recorded and used for calculating the tensile strength. The tensile strength σ_x was calculated by the following formula: $\sigma_x = 2m_s g/\pi dl$, where m_s is the force equivalent mass, g is the gravitational acceleration, d is the compaction diameter (m), and l is the compaction thickness (m) [32]. The mechanical durability of the pellets was measured using a tumbler (Bioenergy TUMBLER 1000+, Austria) following procedures in accordance with ISO 17831–1. The mechanical durability of one pellet is presented as the percentage of the pellet weight remaining after the test and the initial weight. For each pellet sample, the mechanical durability test was carried out at least 3 times, and an average value is presented.

3. Results

3.1. Feedstock

Table 1 shows characteristics of oven-dried birch wood, wood pellet and steam-exploded pellet samples. The proximate analysis results show that all three biomass materials have a high content of volatile matter, above 80 wt%. The ash contents of the three studied biomass materials are low, lower for the wood pellets than for the birch wood chips, and lowest for the steam-exploded pellets, which is as expected since some inorganics are removed in the steam explosion process. The elemental composition of birch wood, wood pellets and steam-exploded pellets are rather similar, with exception of a higher carbon content and a lower oxygen content of the steam-exploded pellets, and the expected higher nitrogen content in birch compared to spruce. The dominant inorganic elements in the three biomass materials are Ca, K, Mg and Mn with small amounts of Si, P and S.

3.2. Biocarbon production and characterization

Table 2 summarizes characteristics of the biocarbon samples produced under different conditions. In comparison to biocarbon produced with purging of N_2, the volatile matter content of the biocarbon produced under constrained conditions are lower. The ash content of the biocarbons produced from the birch wood are in the same range, of 1–2 wt%. The calculated fixed carbon contents of the birch wood biocarbons are also shown in Table 2. Together with the elemental analysis, the calculated fixed-C content of biocarbons indicate that carbonization of birch wood under constrained conditions results in an improvement of carbon conversion efficiency with increase of carbon content of the produced biocarbon. During the biocarbon production process, the biomass feedstock is heated, resulting in thermal decomposition of the feedstock into solid, gases and tarry vapors[5]. For the current work, production of biocarbon without purging gas, with lid on the sample bed and under pressure enables extension of the residence time of the volatiles and tarry vapors in the reactor. It leads to cracking and recondensation of them and forming of secondary carbon. The biocarbons produced under different conditions also have different properties that affect the reactivity of them as described in the following chapter.

3.3. Macro-TGA study

3.3.1. Reactivity

The seven types of biocarbon produced under different conditions from birch wood chips, wood pellets and steam exploded pellets were used for the Macro-TGA study. The goal was to investigate the gasification reactivity of biocarbon produced under different conditions and from woody biomass with and without pelletization treatment under industrially relevant conditions. Fig. 2 shows the loss of fixed carbon of all seven studied biocarbon samples as they reacted as a function of time. It can be seen that the birch wood biocarbons produced at atmospheric pressure has higher reactivities than those produced from the pressurized reactor. However, there are slight differences in fixed carbon loss behaviors of the birch wood biocarbon produced under different conditions in the tubular fixed reactor. For the sample BW500-P that was produced with purging of N_2, it took about 430 s to reach 20% fixed carbon loss. On the other hand, about 480 s was needed for the biocarbon produced by using a lid and no purging gas to realize this. For the biocarbon produced under pressure, it took about 580 s and 610 s for the loss of fixed carbon to reach 20%. Several studies have reported that enhanced biocarbon yields can be obtained by carbonizing biomass under constrained conditions, which causes improvement of fixed carbon content in the produced biocarbon as well [27,26,45,46,50]. Consequently, the produced biocarbons have different properties that affect their conversion behaviours under different atmospheres [47,51]. Our previous work reported micro-TGA experiment results for CO_2 gasification of biocarbon produced under atmospheric and pressurized conditions[4,47]. It was found that the biocarbons produced at high pressures have lower CO_2 reactivity than those produced at atmospheric pressure. Results obtained in the current work showed a similar decreasing trend of reactivity for the biocarbons produced at elevated pressure. In comparison to the biocarbons produced from the birch wood chips, the biocarbons produced from the wood pellets and steam-exploded pellets react slowly under the same Macro-TGA gasification conditions. 826 s and 1160 s were needed for the carbonized wood pellets and carbonized steam-exploded pellets respectively to reach 20%

Table 2
Properties of biocarbon produced under different conditions.

		BW 500-P	BW 500-NPL	BW 350–500-NP	BW-7.9 bar	BW-21.7 bar	WP-500-NP	SP-500-NP
Volatile matter	wt%, d.b.	19.88	15.50	16.81	12.60	11.30	16.77	23.53
Ash content	wt%, d.b.	1.60	2.06	1.06	2.00	1.40	1.02	0.88
Fixed-C*	wt%, d.b.	78.52	82.44	82.13	85.40	87.30	82.21	75.59
C	wt%, daf	78.03	84.18	88.13	90.49	92.62	85.95	88.13
H	wt%, daf	3.68	2.90	2.74	1.93	4.35	2.87	2.74
N	wt%, daf	0.39	0.46	0.43	0.47	0.37	0.37	0.43
S	wt%, daf	0.11	0.06	0.05	0.02	0.02	0.05	0.05
O*	wt%, daf	17.79	12.40	8.66	7.09	2.64	10.76	8.66
K	wt%, d.b.	1269	1918	2040	2469	2208	2330	1960
Ca	wt%, d.b.	2441	6555	3100	3837	3332	3770	2910
P	wt%, d.b.	237	376	350	408	253	250	170
Si	wt%, d.b.	47	68	257	231	221	190	463
Na	wt%, d.b.	10	86	65	73	13	11	11
S	wt%, d.b.	24	45	120	267	210	120	110
Mg	wt%, d.b.	678	961	1006	911	682	551	425
Al	wt%, d.b.	31	50	77	158	72	75	70
Fe	wt%, d.b.	67	87	100	254	70	132	102
Mn	wt%, d.b.	363	565	401	477	344	399	436
Cu	wt%, d.b.	3	5	3	8	3	3	3
Zn	wt%, d.b.	125	258	148	160	120	65	36

d.b.: dry basis; daf: dry ash free basis; *: calculated by difference.

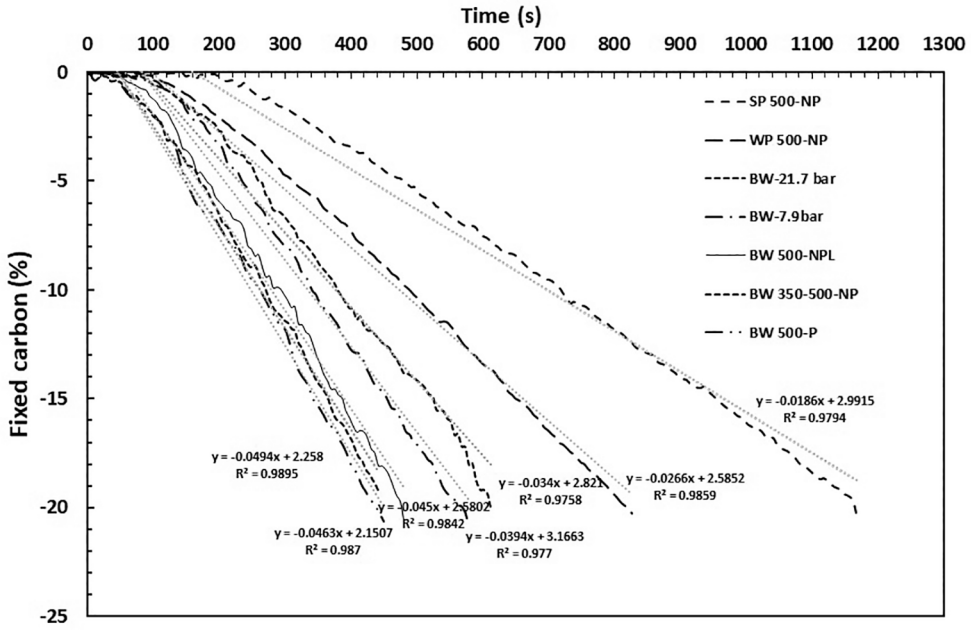

Fig. 2. Fixed carbon loss of biocarbon samples in a mixture of 50 vol% CO_2:50 vol CO at 1100 °C. Biocarbon sample: birch wood (BW), wood pellet (WP) and steam exploded pellet (SP). Production conditions: No N_2 purge (NP), No N_2 purge with a lid on sample bed (NPL), Purge with N_2 (P).

fixed carbon loss. The time used for gasification of carbonized pellets WP-500-NP and SP-500-NP to the desired extent is about 2 and 3 times longer, respectively, than that used for conversion of sample BW-500-P. It is also interesting to see from Fig. 2, that the recorded fixed carbon losses for WP-500-NP and SP-500-NP start later than those of biocarbon produced from the wood chips. It indicates that heat and mass transfer limitations are delaying the onset of the gasification process for the pellets, but also indicates that the biocarbon produced from the pelletized steam-exploded biomass has lower reactivity also due to the lower ash content. The wood pellets used in the current work are produced from virgin spruce wood. Whereas the steam exploded pellets are produced from a mixture of spruce and pine wood. As shown in Table 1, the general properties of the wood pellets and steam exploded pellets are similar to those of the birch wood chips. There are differences in terms of the content of certain inorganic elements contained in these three feedstocks. In addition, in comparison to the birch wood chips, the wood pellets and steam exploded pellets have much higher density with a more compact structure. It will affect pyrolysis behaviors of them and the physio-chemical properties of the produced biocarbon, and reactivity consequently.

Using the slope of the fixed carbon loss curves for the recorded weight measurements during the gasification of the biocarbon, the fraction of reacted fixed carbon per time was calculated. The slope is defined as the gasification reactivity for comparison purpose. As shown in Fig. 3, the sample BW 500-P has the highest reactivity, whereas the biocarbon produced from the steam-exploded pellets has the lowest reactivity.

3.3.2. *Properties of biocarbon after Macro-TGA gasification reaction*

During metal production processes, the carbon reductant will flow through the pre-reduction zone before it reaches the bottom of the smelting furnace to react with metal ore. The properties of the partially

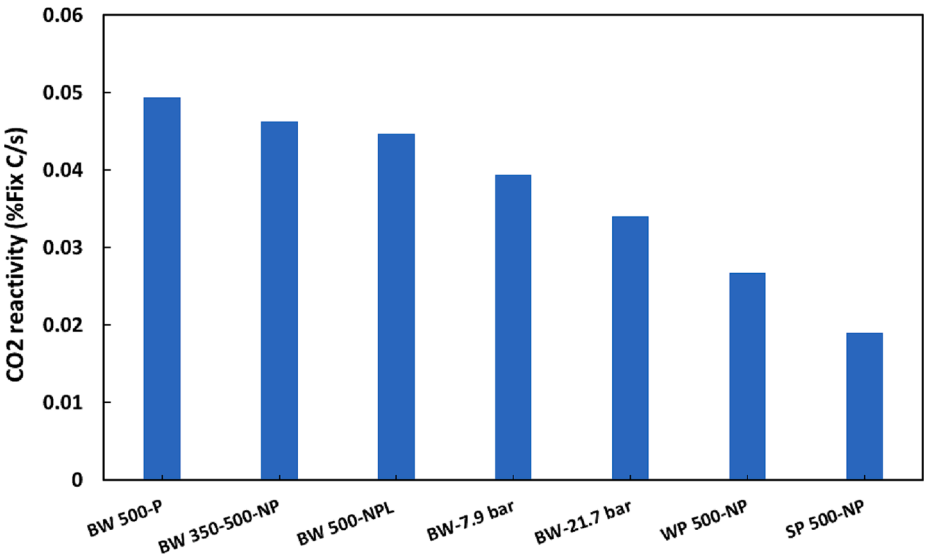

Fig. 3. Gasification reactivity of biocarbon samples in a mixture of 50 vol% CO_2: 50 vol% CO at 1100 °C.

reacted carbon reductant are critical, as they can significantly influence further reactions between it and the metal ore. It is therefore critical to have detailed analyses on the residues from the Macro-TGA gasification tests.

Fig. 4 shows a plot of the O:C against H:C molar ratio of pre-dried biomass materials, biocarbon produced from them and partially reacted biocarbon after Macro-TGA tests. A clear decreasing trend of O:C and H:C molar ratio can be seen in Fig. 4. As shown in Fig. 4, the raw biomass materials have high O:C and H:C molar ratios that is indicated with a green ellipse in the right upper corner. The O:C and H:C molar ratios of biocarbon produced at 500 °C decreased to the range of 0.05–0.2 and 0.2–0.6 (highlighted with a red ellipse), respectively. After gasification experiments, the O:C and H:C molar ratios of biocarbon further decrease and all are smaller than 0.1, as highlighted by a light blue ellipse in the left bottom corner in Fig. 4. The change of O:C and H:C molar ratios as shown in Fig. 4 is mainly related to decomposition of biomass during carbonization and further loss of volatiles during the Macro-TGA tests. The increase of carbon content and reduction of hydrogen content agree well with the findings reported by Ueki et al., when the woody biomasses were thermally treated at elevated temperature from 300 to 1000 °C [43].

Table 3 summarizes results for analyses of inorganic elements in the residual biocarbon after the Macro-TGA gasification tests. The analysis results showed that Ca, K and Mg are dominant elements in the partially reacted biocarbon with detection of certain amounts of Si, Mn, P and Fe, and minor amounts of Na, S and Al. It can be seen from Table 3 that the concentration of most inorganic elements in the biocarbon produced under atmospheric pressure with using a lid and from the pressurized reactor are higher than those in sample BW 500-P. With using a lid on the sample bed, the tarry vapors and gas products released away from the reactor were considerably delayed and also reduced, which is more evident for the pressurized carbonization process. It leads to more intensive cracking of tarry vapors that deposit or condense on the charring biomass particle surfaces, resulting in blocking of pores and limiting migration of inorganic elements from the inner structure to the external surface [49]. On the other hand, slow carbonization with

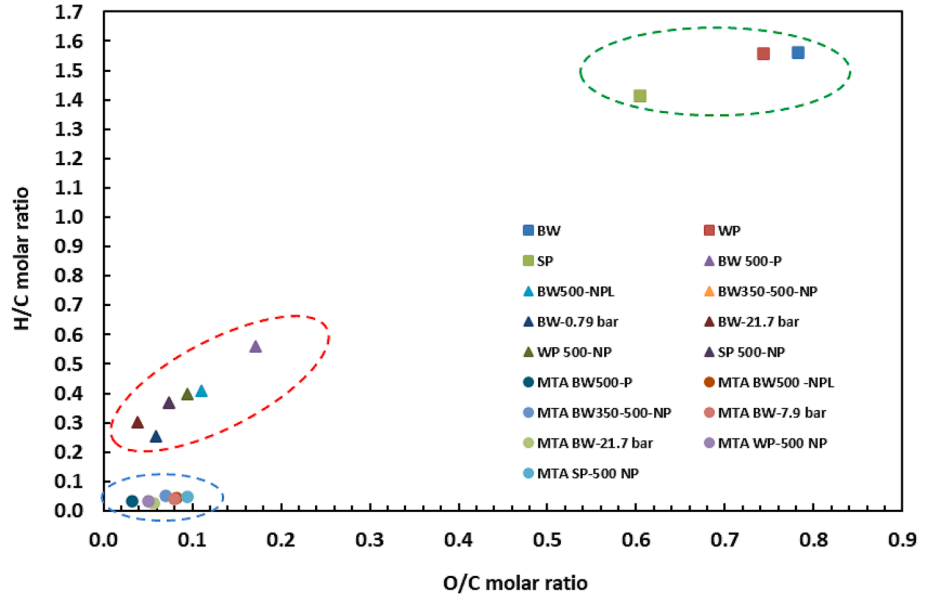

Fig. 4. Comparison of Van Krevelen diagram of pre-dried biomass materials, biocarbon from birch wood chips, wood pellets and steam exploded pellets and the residual biocarbon after the Macro-TGA tests (i.e., devolatilized at 1100 °C, and having further lost 20% of its remaining mass).

Table 3
Inorganic elements in biocarbon after Macro-TGA (MTA) gasification reactions (mg/kg, wt%,d.b.).

	MTA BW 500-NP	MTA BW 500-NPL	MTA BW 350–500-NP	MTA BW-7.9 bar	MTA BW-21.7 bar	MTA WP-500-NP	MTA SP-500-NP
K	1900	4900	4370	5680	5560	6170	2820
Ca	4310	7610	6390	8410	6190	4670	4030
P	360	780	650	880	510	310	260
Si	176	435	261	241	600	175	238
Na	80	86	91	101	61	238	69
S	31	70	80	44	34	90	50
Mg	832	1500	1863	1915	874	641	624
Al	25	159	31	40	100	62	73
Fe	195	167	204	304	288	88	148
Mn	159	697	387	480	534	410	332
Cu	7	8	7	11	11	6	5
Zn	2	5	2	2	3	2	1

purging of N_2 causes more intensive heat and mass transfer within and at the external surface of charring biomass particles, leading to formation of biocarbon with a more porous structure [3,13]. It favors the migration and release of inorganic elements.

During the Macro-TGA gasification experiments, devolatilization and further gasification of the biocarbon samples took place. As shown in Table 3, the absolute concentration of inorganic elements in the partially reacted biocarbon is increased as a result of the consumption of carbon. The high concentrations of elements, for example, K and P, in the partially reacted biocarbon need to be carefully considered. These inorganic elements is prone to involve in reactions between the biocarbon and metal ore and slag in the reduction zone of a smelting furnace, which can affect properties of the final products [17].

3.3.3. SEM-EDX analysis

Figs. 5-11 show SEM images taken from the seven biocarbon samples before and after the Macro-TGA gasification experiments with increasing magnifications. One should note that the EDX analyses are only qualitatively indicating the concentration of detected elements. Together with bulk analysis of inorganic elements in one studied sample, an abundance of certain elements in the same detected spots or areas implies the presence of chemicals or compounds (i.e., calcium oxide or calcium carbonate). A similar method has been used in other works to investigate transformation of inorganic elements (i.e., alkali metals) during thermal conversion of biomass materials [9,40]. Considerable differences in surface morphology and microstructure can be observed for the biocarbons produced under different conditions. As shown in Fig. 5(a and b), the sample BW 500-P has a porous structure and coarse surface with visible large openings and cracks. On the other hand, the samples BW 500-NLP (Fig. 6(a and b)) and BW 350–500 NP (Fig. 7(a and b)) have a more compact structure and much fewer cracks and pores can be observed. The sample BW 500-NLP has a much smoother surface without showing the fiber structure as observed for BW 500-P. Additionally, a bubble-like structure can be found in Fig. 5(b), indicting formation of a carbon layer due to cracking and condensation of tarry vapors as a result of constrained carbonization conditions. The biocarbon produced under pressures have evidently different microstructure than those produced at atmospheric pressure. Figs. 8 and 9 show that biocarbon produced at respectively 7.9 and especially 21.7 bar underwent a molten stage with forming and cracking of bubbles, without showing the cellular and fiber structure that normally can be found. Similar microstructure and morphology of biocarbon produced under pressurized conditions have been reported in our previous studies [21–22,45,50]. The biocarbon samples produced from the wood pellets and steam exploded pellets, as shown in Figs. 10 and 11, have dense structure compared to the biocarbon produced from wood chips. Fig. 10 (b) shows a zoom-in view of the scanned area of one carbonized wood pellet that is formed due to binding of crushed wood particles. Different than the carbonized wood pellet WP-500-NP, Fig. 11(a and b) show that the carbonized steam-exploded pellet SP-500-NP has a much denser structure and more intact surface without showing a clear fibrous structure. The SEM analyses were conducted on the biocarbon after Macro-TGA gasification experiments. Figs. 5-7 show that, in comparison to unreacted biocarbon, the biocarbon samples after gasification experiments have coarser surfaces with particles and grains in different sizes that can be observed on their surface. It is more evident for the sample BW 500-NPL. Fig. 6(c and d) clearly show that, in comparison to the unreacted sample, more cracks formed on the surface of reacted

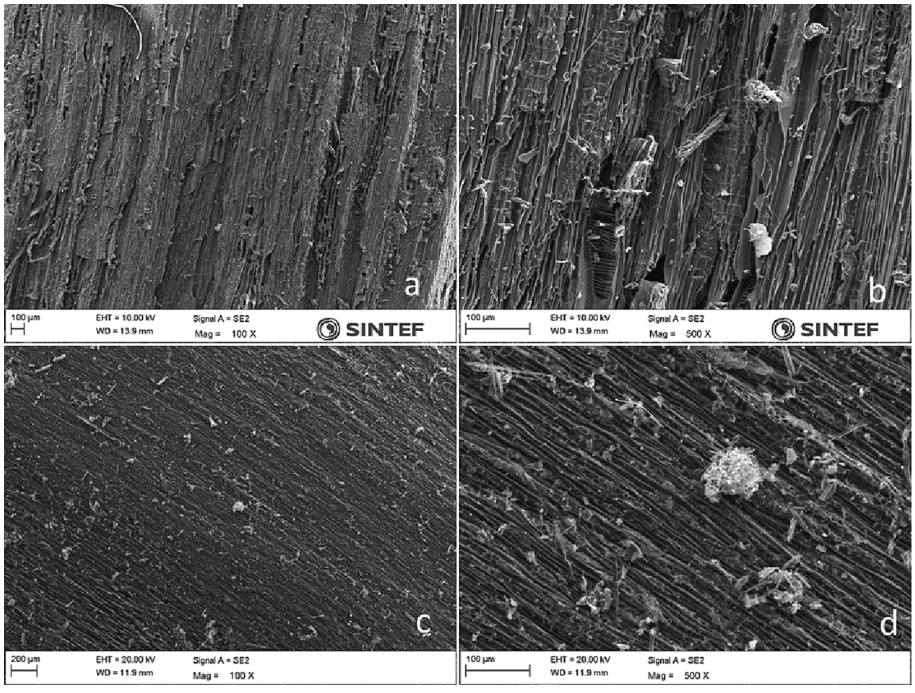

Fig. 5. SEM images of biocarbon BW 500-NP before (a, b) and after (c, d) Macro-TGA gasification reaction.

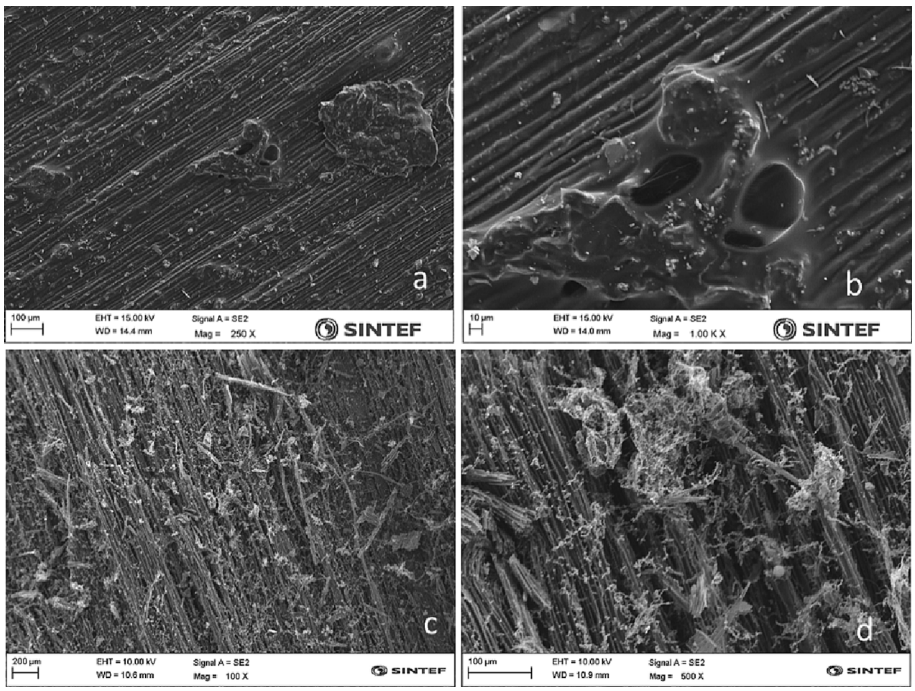

Fig. 6. SEM images of biocarbon BW 500-NPL before (a, b) and after (c, d) Macro-TGA gasification reaction.

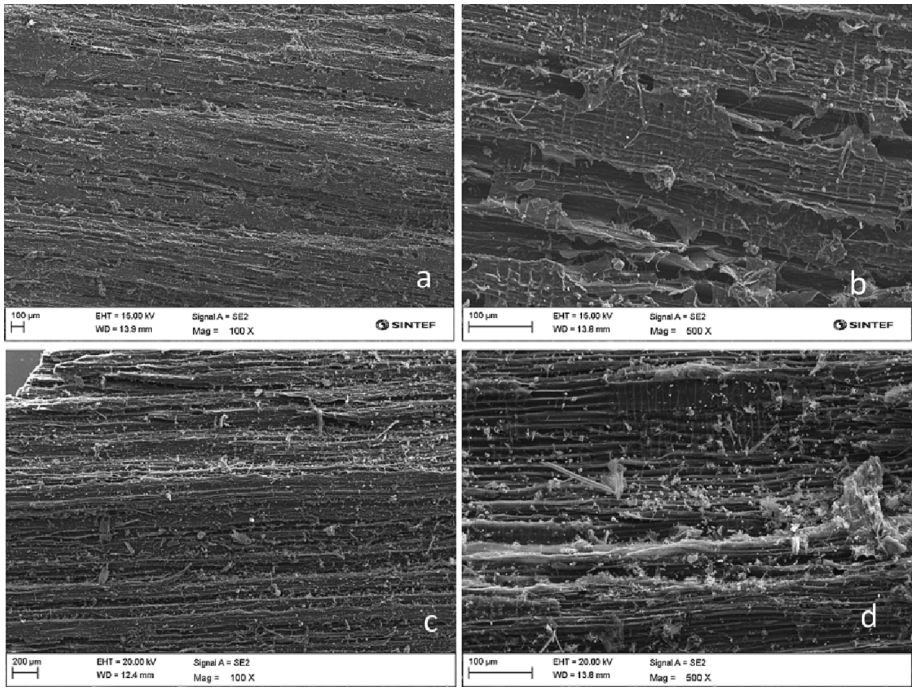

Fig. 7. SEM images of biocarbon BW 350–500-NP before (a, b) and after (c, d) Macro-TGA gasification reaction.

biocarbon with presence of agglomerated grains and long thread-like structures. As shown in Figs. 10 and 11, the reacted carbonized WP-500-NP and SP-500-NP preserved dense structure. However, for the reacted WP-500-NP, there are large numbers of small openings and several large cracks that can be observed (Fig. 10(d)). Differences in surface morphologies of raw and reacted biocarbon samples indicate reactions of them during Macro-TGA gasification experiments. The biocarbons produced at atmospheric conditions are distinguished by coarser surfaces with more and larger openings and cracks. It is related to the high conversion level of the biocarbons as more intensive reactions cause consumption of carbon and release of formed gas products [25].

Figs. 12-18 display detailed SEM-EDX analyses on the seven biocarbon samples after the Macro-TGA experiments. One should note that the EDX analyses are only qualitative indicating the concentration of detected elements. Together with bulk analysis of inorganic elements in one studied sample, an abundance of certain elements in the same detected spots or areas implies the presence of chemicals or compounds (i.e., calcium oxide or calcium carbonate). A similar method has been used in other work to investigate transformation of inorganic elements

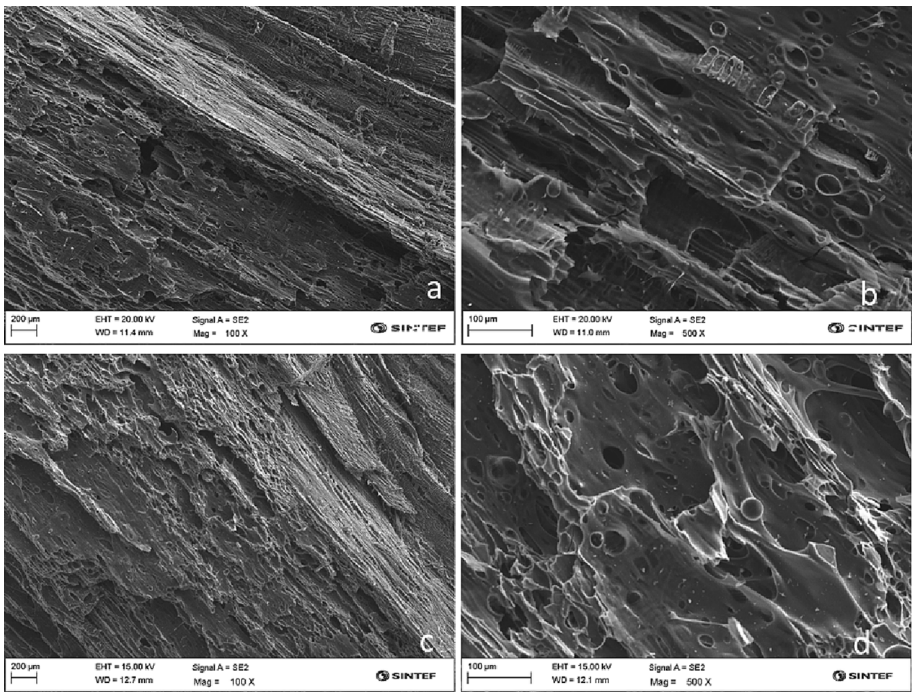

Fig. 8. SEM images of biocarbon BW-7.9 bar before (a, b) and after (c, d) Macro-TGA gasification reaction.

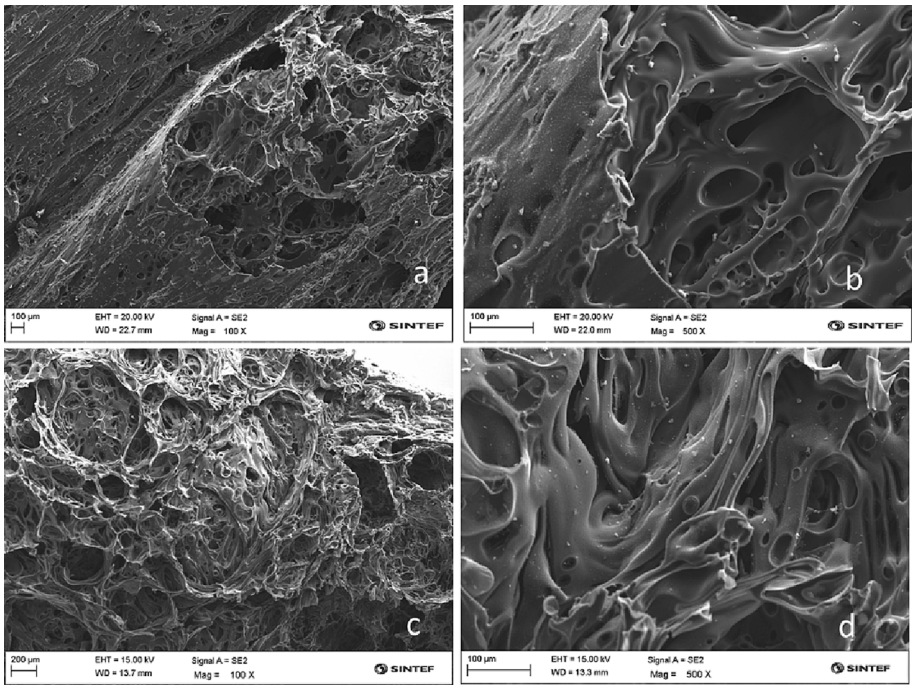

Fig. 9. SEM images of biocarbon BW-21.7 bar before (a, b) and after (c, d) Macro-TGA gasification reaction.

(i.e., alkali metals) during thermal conversion of biomass materials. [9,40] For the biocarbon produced at atmospheric conditions, there are evident migration and agglomeration of inorganic elements. Fig. 12 shows a white-grey aggregate on the surface of the gasified sample BC-500-P, which has a porous structure with small bead-like particles that can be observed (Fig. 12(a)). The EDX analysis results (Fig. 12(d)) show that Ca is the dominant inorganic element detected from the aggregate, with smaller amounts of Fe, K and Mg and P. The elements C and O are also detected as major elements in the aggregate, indicating presence of calcium carbonate. EDX spot analysis was also conducted on the bulk part of the gasified sample BW 500-P. Only minor amounts of Ca, Fe and K were detected as main inorganic elements. For the gasified sample BW 500-NPL, the aggregates (Fig. 13(a)) with similar structures can be observed, which has similar chemical composition as detected from the gasified BW 500-P. For the gasified biocarbon sample BW-7.9 bar and BW-21.7 bar, smaller white grains can be observed on their surface. Ca was detected as a main inorganic element. However, the content of other inorganic elements such as K, P and Fe are much lower than those detected from the gasified biocarbon samples BW 500-P and BW 500-NPL, indicating different transformation chemistry and migration

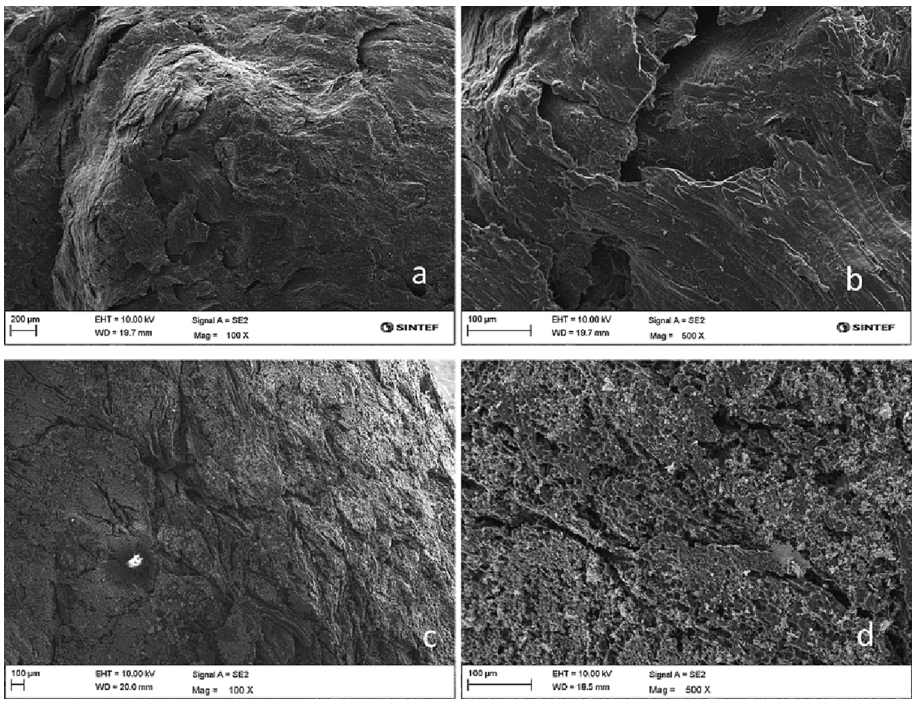

Fig. 10. SEM images of biocarbon WP-500-NP before (a, b) and after (c, d) Macro-TGA gasification reaction.

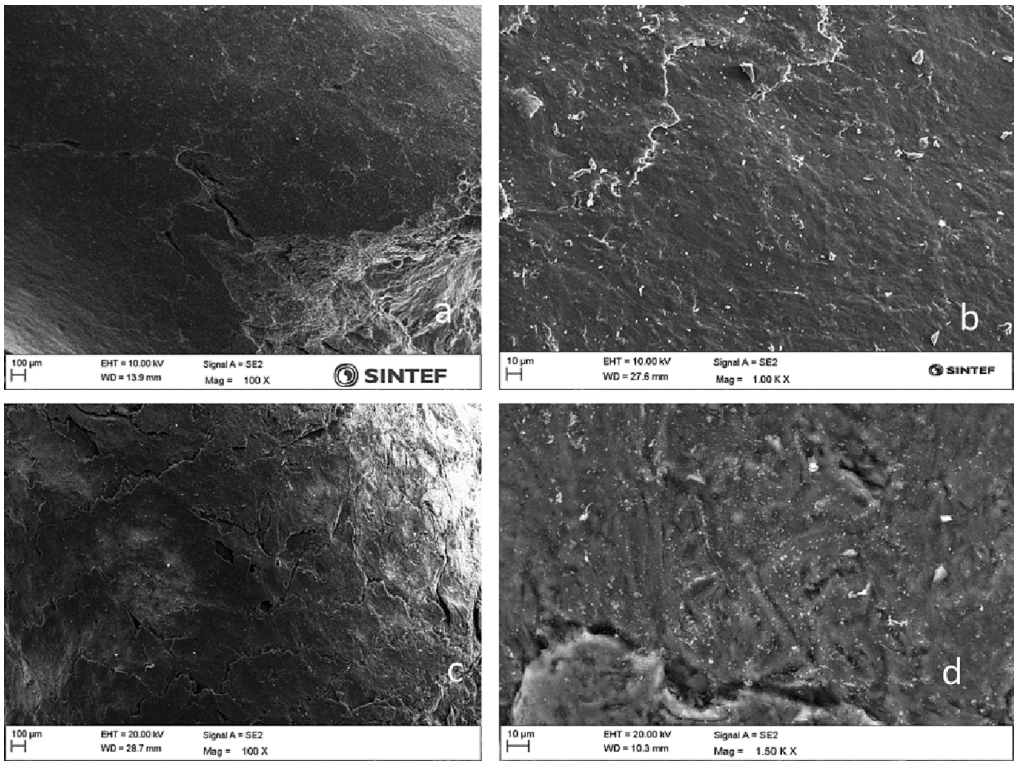

Fig. 11. SEM images of biocarbon SP-500-NP bar before (a, b) and after (c, d) Macro-TGA gasification reaction.

behaviors of these elements. For the gasified sample WP-500-NP, tiny white particles can be observed on its surface (spot 3, Fig. 17(a)) and some of them agglomerate together into a flake-like grain (spot 4, Fig. 17 (a)). Ca was detected the main element in these particles and grains with minor amounts of Si, Al and Mg (Fig. 17(b)). The SEM-EDX results shown in Figs. 12-18 imply different migration and transformation behaviors of inorganic elements during Macro-TGA gasification of biocarbon produced under different conditions and from different feedstocks. For biocarbon produced under atmospheric pressure, more intensive migration of inorganic elements occurred during the gasification process, which accumulate and aggregate on the external surface of the biocarbon. On the other hand, less amounts of inorganic elements were observed and detected on the external surface of biocarbon samples that were produced under pressure. The SEM-EDX analyses imply

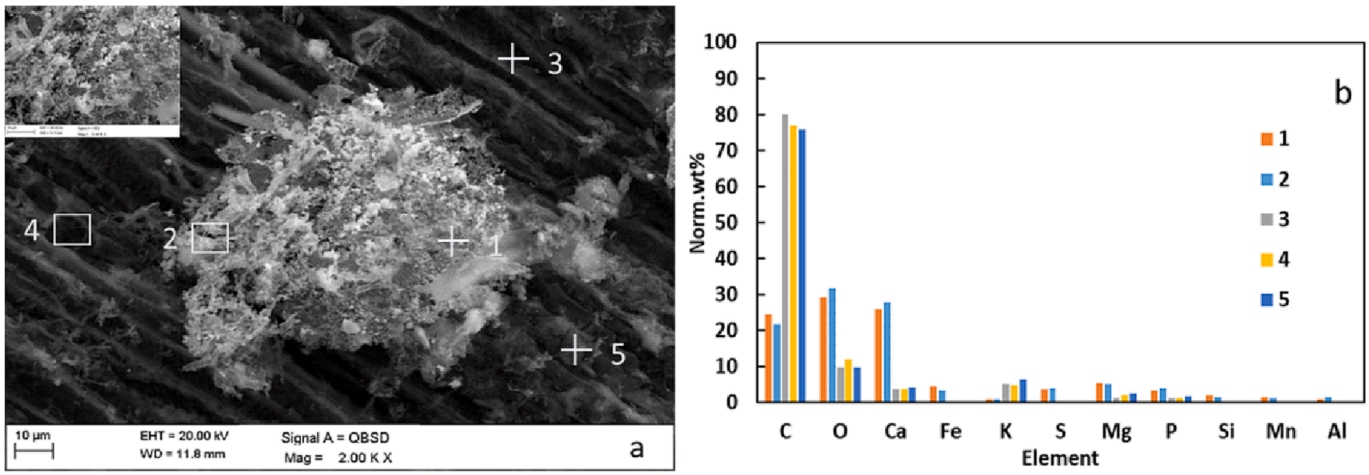

Fig. 12. SEM image (a) and EDX spot analysis (b) of biocarbon BW 500-NP after Macro-TGA gasification reaction.

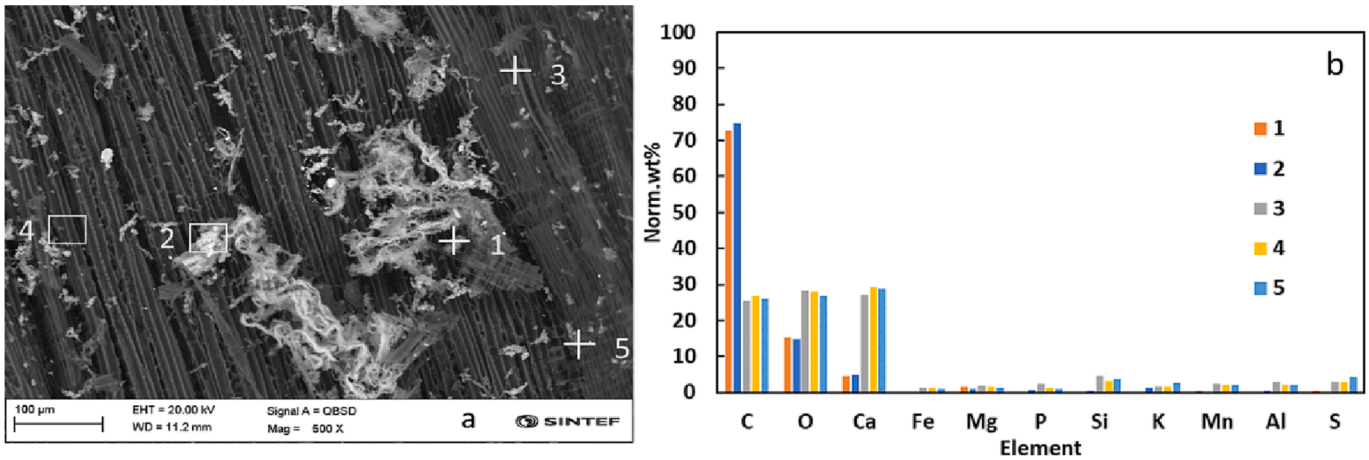

Fig. 13. SEM image (a) and EDX spot analysis (b) of biocarbon BW 500-NPL after Macro-TGA gasification reaction.

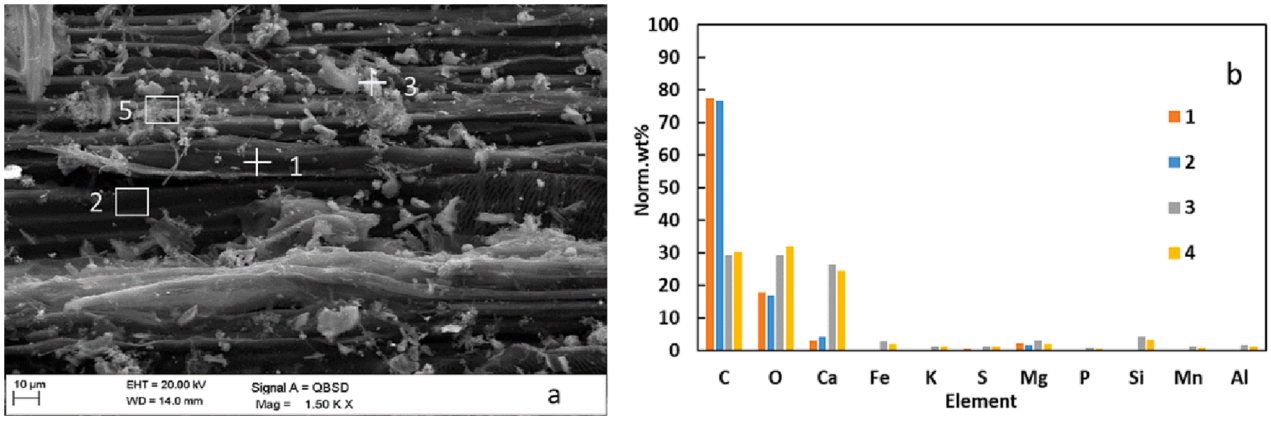

Fig. 14. SEM image (a) and EDX spot analysis (b) of biocarbon BW 350–500-NP after Macro-TGA gasification reaction.

that inorganic elements have a higher potential to migrate to external surfaces of the biocarbon during gasification of sample BW 500-P, which has more open and porous structure. On the other hand, transformation and movement of inorganic elements in the biocarbon produced under pressure and from biomass pellets are much less intensive. The inorganic elements, especially Ca, can promote the Boudouard reaction through acting as catalysts and enhance gasification rate of the biocarbon. Migration and diffusion of inorganic elements can initiate formation and further growth of pores in the carbon structure and on the external carbon surface. It causes increase of porosity and surface area of the carbon, which again promotes the gasification of biocarbon [36]. As the inorganic elements migrate to the external surface of the biocarbon, they will also promote the Boudouard reaction through acting as catalysts. The dispersion and presence of inorganic elements on biocarbon

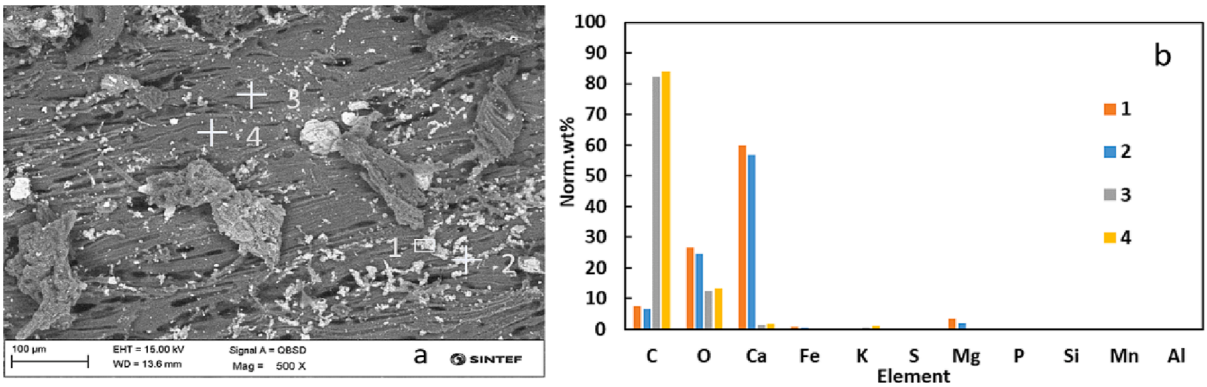

Fig. 15. SEM image (a) and EDX spot analysis (b) of biocarbon BW-7.9 bar after Macro-TGA gasification reaction.

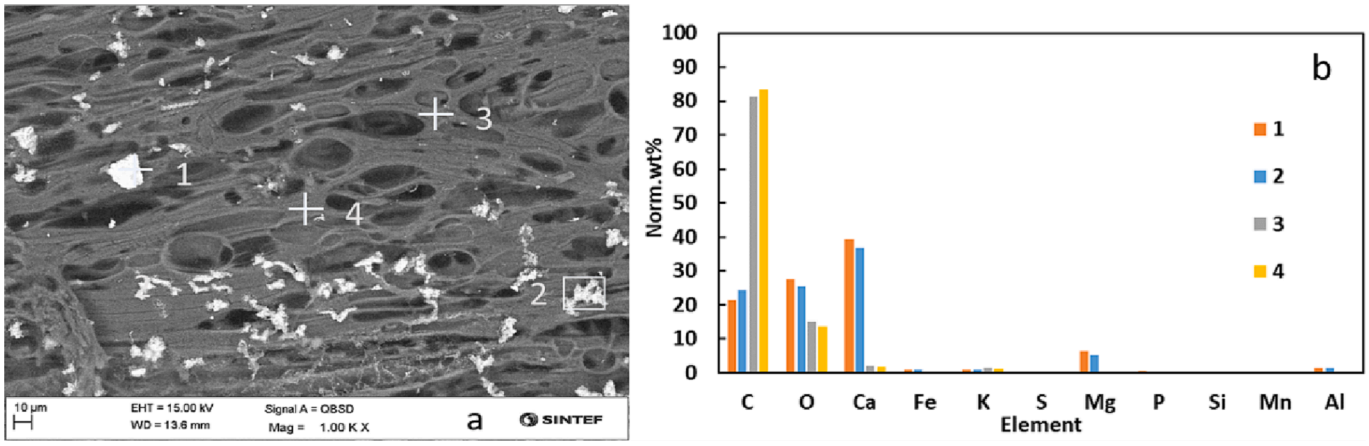

Fig. 16. SEM image (a) and EDX spot analysis (b) of biocarbon BW-21.7 bar after Macro-TGA gasification reaction.

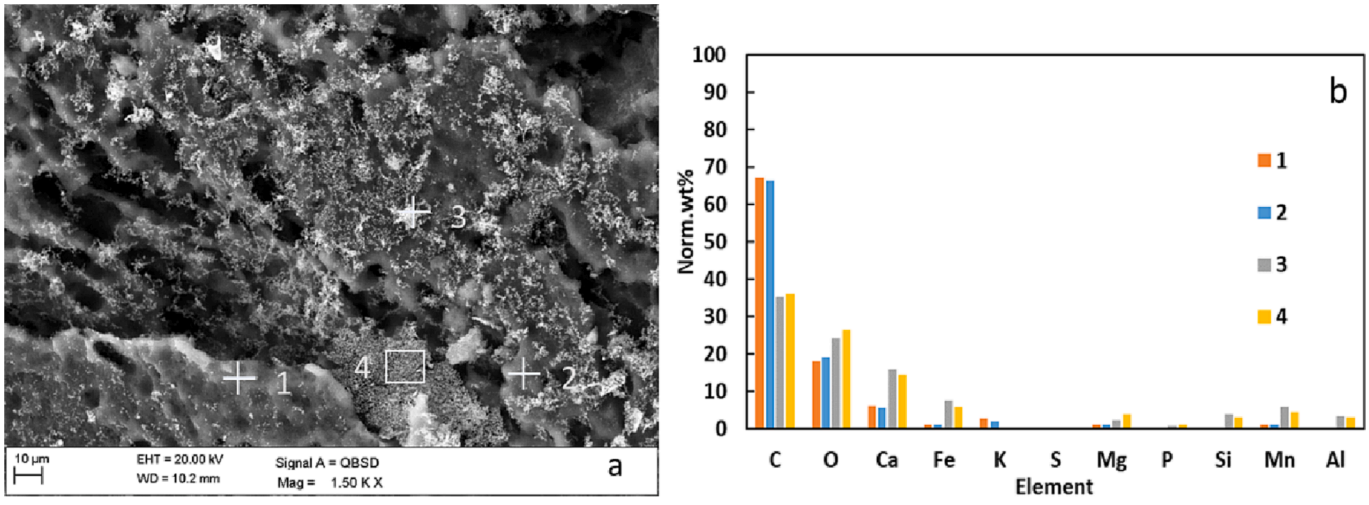

Fig. 17. SEM image (a) and EDX spot analysis (b) of biocarbon WP 500-NP after Macro-TGA gasification reaction.

surfaces will provide active sites, which can play catalytic roles to lower the activation energy of gasification reactions that take place on the carbon surface [8,19,35]. Presence of the catalytic inorganic elements speeds up the gasification reactions in the carbon matrix, which shifts progressively towards the particle periphery. The consumption of carbon and release of intermediate gas products cause reduction of density and mechanical stability of the biocarbon. The SEM-EDX analysis results agree with previous findings about dispersion of inorganic elements (i.e., Ca and K) during CO_2 gasification of biocarbon and coke, which increased gasification reactivity and promoted conversion of the studied samples [23,36].

3.3.4. µCT analysis of biocarbon before and after Macro-TGA gasification reaction

Figs. 19-22 show µCT scanning results of biocarbon before and after the Macro-TGA gasification test. The biocarbon produced under

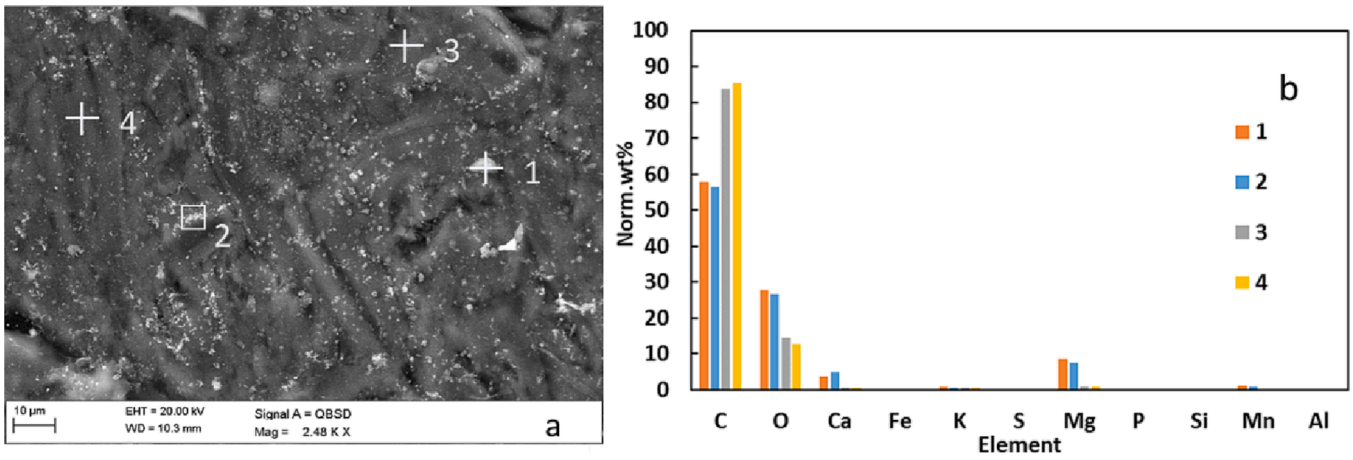

Fig. 18. SEM image (a) and EDX spot analysis (b) of biocarbon SP 500-NP after Macro-TGA gasification reaction.

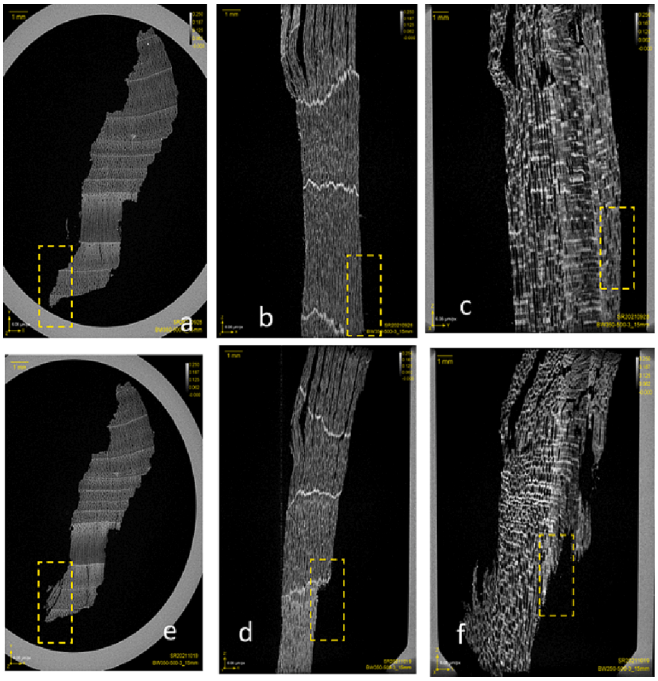

Fig. 19. µCT analysis of BW-350-500-NP before (a-c) and after Macro-TGA gasification reaction (e-f).

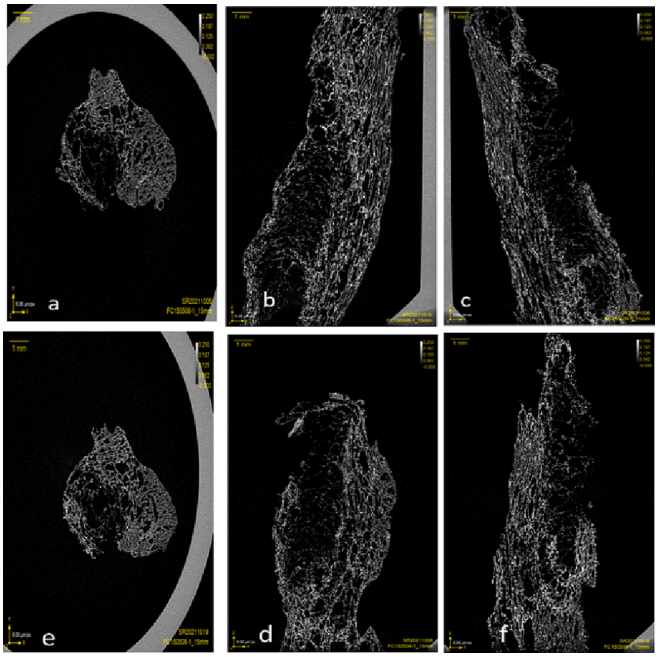

Fig. 20. µCT analysis of BC-21.7 bar before (a-c) and after Macro-TGA gasification reaction (e-f).

atmospheric conditions (BW-350-500-NP) preserves a fibrous structure. Whereas the biocarbon produced under 21.7 bar has a swollen round shape seen in the horizontal direction. In addition, large voids and hollow structures of the biocarbon grain can be seen in all scanned directions. The sample SP-500-NP has a dense and compact structure without identification of individual grains or particles.

After the Macro-TGA gasification experiments, the biocarbon grains have shrunk as seen from images scanned from different directions. As shown in Fig. 19(e and f), the consumption of sample BW 350–500-NP can be observed mainly at the edges or tips of the biocarbon grains, as indicated with yellow rectangles.

µCT analysis of sample WP-500-NP is shown in Fig. 21. Compared to the unreacted pellet, there is clear shrinkage of it after gasification reaction and the rim of the exterior pellet is uneven. The general structure of the reacted pellet became less dense and several big cracks can be clearly seen from Fig. 21(d, e and f). During the Macro-TGA gasification experiment, devolatilization and decomposition of the pellet takes place, which results in formation of volatiles and gaseous products. Further release of them from the inner part of the pellets will further cause formation of cracks inside and on the external surface of WP-500-NP. On the other hand, the reacted sample SP-500-NP preserved the initial shape with only a slight reduction of size, and kept its dense and compact structure. The differences in the µCT analysis on the reacted WP-500-NP and SP-500-NP imply that WP-500-NP is more reactive during the gasification test, agreeing with the results in section 3.3.1.

3.3.5. Mechanical properties analysis of raw, carbonized and gasified in the Macro-TGA

Mechanical strength is among the most important metrics of the biocarbon, as used for metallurgical industry applications [33,42]. In previous work, only the mechanical properties of raw and carbonized biomass pellets were studied. To the best of our knowledge, our work is the first one to study and report key mechanical properties of carbonized biomass pellets after gasification at a high temperature in a gas mixture of CO and CO_2. Fig. 23(a) shows that the steam exploded pellets have a much higher compressive strength than the wood pellets. Evident differences in mechanical strength between normal wood pellets and

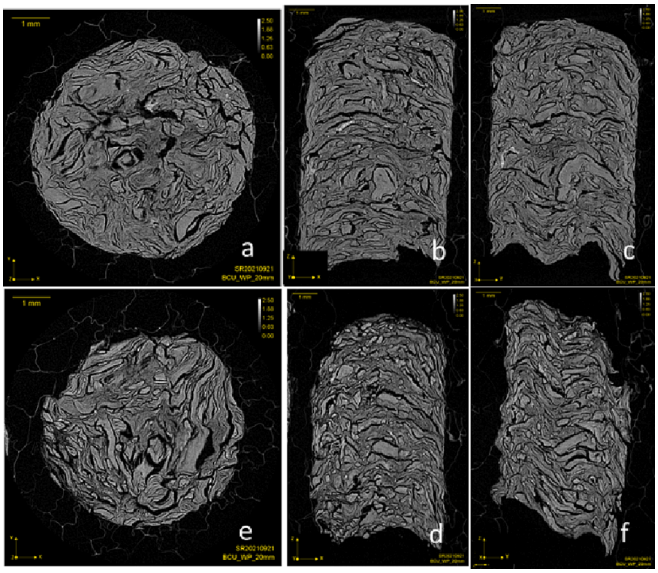

Fig. 21. μCT analysis of WP-500-NP before (a-c) and after Macro-TGA gasification reaction (e-f).

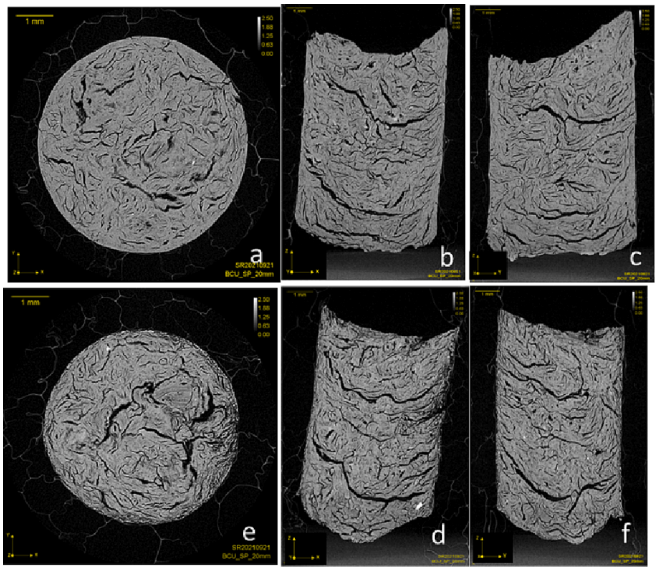

Fig. 22. μCT analysis of SP-500-NP before (a-c) and after Macro-TGA gasification reaction (e-f).

pellets produced from steam exploded wood have been reported in several studies [1,7,20]. During the steam explosion treatment at mild temperature and high pressure, lignin in the biomass is softened and released from the biomass cell wall and distributed onto the particle surfaces [55]. Normally, the steam exploded biomass material is directly fed into a pellet mill, where it is again exerted under pressure. The lignin on particle surfaces will act as adhesive binder to bond steam exploded biomass particles together, promoting formation of pellets with higher durability, stiffness and water resistance [2]. Fig. 23(a) shows that compressive strength of the studied pellets decreases drastically upon carbonization at 500 °C and further gasification reaction at 1100 °C. The steam exploded pellets after carbonization and further gasification reaction still have superior compressive strength compared to the wood pellets after the same conversion. However, the differences become smaller. Fig. 23(b) shows that the wood pellets and steam exploded pellets have similar mechanical durability. Upon carbonization treatment, the mechanical durability of the wood pellets decreased considerably from 96% to 58%. With further gasification reaction, the durability of the carbonized wood pellets decreased slightly further. It is interesting to see that the steam exploded pellets had a much better mechanical durability, which only reduced from 98% to 82%, even after gasification reaction at 1100 °C. The mechanical strength and durability of biomass pellets are mainly related to physical bonding forces between particles in the pellets. During the carbonization process, degradation of the main composition of biomass (i.e., hemicellulose, cellulose and lignin polymers) takes place. It results in weakening and cleavage of covalent bonds between the matrix and these polymers encrusting cell fibrils and loss of bonds between them. In addition, decomposition of these polymers leads to generation of water and volatiles. Formation and release of them will further result in formation of voids in and between particles in the pellets, reducing contacts and adhesive forces between particles [7]. Therefore, the evident reduction of mechanical strength of both wood pellets and steam exploded pellets is mainly related to a combination of the decomposition of biological components and a decrease of bonds between individual particles. For one gasification test, the carbonized pellets were first calcinated at 1100 °C for half an hour, followed by gasification in a gas mixture of CO_2 and CO. Therefore, the measured mechanical properties of the wood pellets and steam exploded pellets are a consequence of both devolatilization and partial gasification. In comparison to the steam exploded pellets, the wood pellets have lower bulk density as shown in Fig. 20(a). The carbonized wood pellet (WP-500-NP) has a higher reactivity than the carbonized steam exploded pellet (SP-500-NP). More intensive gasification reactions can be expected for WP-500-NP which results in further decrease of its density and formation of voids and cracks as shown in Fig. 21(f). In addition, as discussed in section 3.3.3, there is clear redistribution and migration of inorganic elements from the carbon matrix to the external surface. This will probably also lead to creation of weak spots and enhance anisotropy of the mechanical properties of WP-500-NP. Similar physical influences of mineral compounds on mechanical strength of coke has been reported by Gornostayev et al. [11]. Therefore, in comparison to SP-500-NP, the low mechanical strength of WP-500-NP can be partially explained by the more intensive gasification reactions and transformation of the inorganic elements during gasification of it.

4. Conclusion

In this work, biocarbon was produced from wood chips and pellets under atmospheric and pressurized conditions. The CO_2 gasification reactivity of the produced biocarbons was studied by using a Macro-TGA at conditions relevant to those of industrial furnaces for manganese alloy production. The raw and reacted biocarbons were analyzed in terms of general properties, concentration of inorganic elements, microstructure/chemistry and mechanical strength. It was found that biocarbons produced under different conditions have different CO_2 gasification reactivities. Biocarbon produced from an atmospheric slow heating rate carbonization process has the highest CO_2 reactivity, followed by biocarbons produced from a staged pyrolysis process and in a pressurized carbonization process. Biocarbon produced from steam exploded pellets has the lowest gasification reactivity. It was also found that transformation and release behaviors of inorganic elements in the studied biocarbons are different. In the current work, the reactivity of the studied biocarbons is related to their physio-chemical properties (i.e., microstructure and concentrations of inorganic elements) and transformation behaviors and catalytic effects of the inorganic elements during the gasification process. Higher gasification reactivities were observed for the biocarbon samples with more porous and open structure. This structure favors heat and mass transfer processes during the gasification experiment and consumption of carbon consequently. In addition, inorganic elements in the biocarbon will also play a catalytic role and promote gasification reactions of biocarbon. It partially explains a higher gasification reactivity of some biocarbons as reported in the current work. The mechanical properties of the wood pellets and

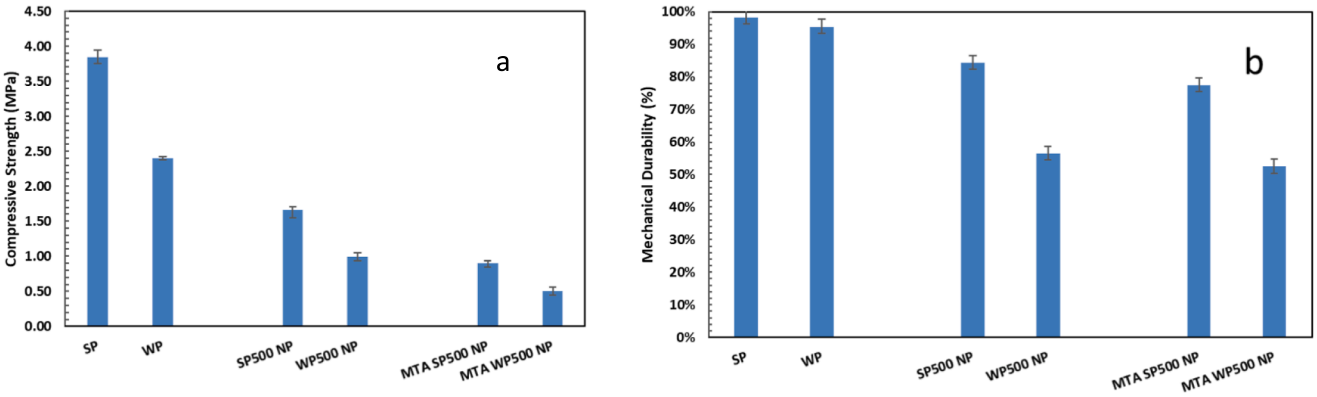

Fig. 23. Tensile compressive strength (a) and mechanical durability (b) of pre-dried, carbonized wood pellet and steam exploded pellet and residual pellets after Macro-TGA gasification experiment.

steam exploded pellets are considerably changed upon carbonization and further gasification in the Macro-TGA. The compressive strength of the carbonized wood pellets drastically decreased after gasification at given conditions, indicating low capacity to withstand cracking or breaking due to static and dynamic crushing force.

Declaration of Competing Interest

The authors declare that they have no known competing financial interests or personal relationships that could have appeared to influence the work reported in this paper.

Data availability

Data will be made available on request.

Acknowledgments

The authors acknowledge the financial support from the Research Council of Norway and the BioCarbUp project industry partners: Elkem AS – Department Elkem Technology, Eramet Norway AS, Norsk Biobrensel AS, Eyde Cluster, Hydro Aluminium AS, and Alcoa Norway ANS.

References

[1] Alizadeh P, Dumonceaux T, Tabil LG, Mupondwa E, Soleimani M, Cree D. Steam Explosion Pre-Treatment of Sawdust for Biofuel Pellets. Clean Technol 2022;4:1175–92. https://doi.org/10.3390/cleantechnol4040072.
[2] Barta-Rajnai E, Wang L, Sebestyén Z, Barta Z, Khalil R, Skreiberg Ø, et al. Comparative study on the thermal behavior of untreated and various torrefied bark, stem wood, and stump of Norway spruce. Appl Energy 2017;204:1043–54. https://doi.org/10.1016/j.apenergy.2017.05.057.
[3] Branca C, Giudicianni P, Di Blasi C. GC/MS Characterization of Liquids Generated from Low-Temperature Pyrolysis of Wood. Ind Eng Chem Res 2003;42:3190–202. https://doi.org/10.1021/ie030066d.
[4] Bui HH, Wang L, Tran KQ, Skreiberg Ø. CO2 gasification of charcoals produced at various pressures. Fuel Process Technol 2016;152:207–14. https://doi.org/10.1016/j.fuproc.2016.06.033.
[5] Chen D, Cen K, Zhuang X, Gan Z, Zhou J, Zhang Y, et al. Insight into biomass pyrolysis mechanism based on cellulose, hemicellulose, and lignin: Evolution of volatiles and kinetics, elucidation of reaction pathways, and characterization of gas, biochar and bio-oil. Combust Flame 2022;242:112142. https://doi.org/10.1016/j.combustflame.2022.112142.
[6] Chen J, Ren W, Guo Y, Zhang S. Degradation of Structure and Properties of Coke in Blast Furnace: Effect of High-Temperature Heat Treatment. In: Zhang M, Li J, Li B, Monteiro SN, Ikhmayies S, Kalay YE, et al., editors. Charact. Miner. Met. Mater. 2022, Cham: Springer International Publishing. 2022. 163–75.
[7] Chen W-H, Peng J, Bi XT. A state-of-the-art review of biomass torrefaction, densification and applications. Renew Sustain Energy Rev 2015;44:847–66. https://doi.org/10.1016/j.rser.2014.12.039.
[8] Di Blasi C. Combustion and gasification rates of lignocellulosic chars. Prog Energy Combust Sci 2009;35:121–40. https://doi.org/10.1016/j.pecs.2008.08.001.
[9] Fagerström J, Steinvall E, Boström D, Boman C. Alkali transformation during single pellet combustion of soft wood and wheat straw. Fuel Process Technol 2016;143:204–12. https://doi.org/10.1016/j.fuproc.2015.11.016.
[10] Feng B, Bhatia SK. Variation of the pore structure of coal chars during gasification. Carbon 2003;41:507–23. https://doi.org/10.1016/S0008-6223(02)00357-3.
[11] Gornostayev SS, Härkki JJ. Mechanism of Physical Transformations of Mineral Matter in the Blast Furnace Coke with Reference to Its Reactivity and Strength. Energy Fuels 2006;20:2632–5. https://doi.org/10.1021/ef060147x.
[12] Greco G, Videgain M, Di Stasi C, Pires E, Manyà JJ. Importance of pyrolysis temperature and pressure in the concentration of polycyclic aromatic hydrocarbons in wood waste-derived biochars. J Anal Appl Pyrolysis 2021:159. https://doi.org/10.1016/j.jaap.2021.105337.
[13] Hu Q, Cheng W, Mao Q, Hu J, Yang H, Chen H. Study on the physicochemical structure and gasification reactivity of chars from pyrolysis of biomass pellets under different heating rates. Fuel 2022;314:122789. https://doi.org/10.1016/j.fuel.2021.122789.
[14] Jayasekara AS, Monaghan BJ, Longbottom RJ. The kinetics of reaction of a coke analogue in CO2 gas. Fuel 2015;154:45–51. https://doi.org/10.1016/j.fuel.2015.03.053.
[15] Kaczorowski J, Lindstad T, Syvertsen M. The Influence of Potassium on the Boudouard Reaction in Manganese Production. ISIJ Int 2007;47:1599–604. https://doi.org/10.2355/isijinternational.47.1599.
[16] Kaffash H, Surup GR, Tangstad M. Densification of Biocarbon and Its Effect on CO2 Reactivity. Processes 2021;9:193. https://doi.org/10.3390/pr9020193.
[17] Kaffash H, Tangstad M. CO2 Gasification of Densified Biomass: The Influence of K on Reaction Rate. JOM 2022;74:1900–7. https://doi.org/10.1007/s11837-021-05150-7.
[18] Kamal Baharin NS, Koesoemadinata VC, Nakamura S, Azman NF, Muhammad Yuzir MA, Md Akhir FN, et al. Production of Bio-Coke from spent mushroom substrate for a sustainable solid fuel. Biomass Convers Biorefinery 2022;12:4095–104. https://doi.org/10.1007/s13399-020-00844-5.
[19] Karlström O, Dirbeba MJ, Costa M, Brink A, Hupa M. Influence of K/C Ratio on Gasification Rate of Biomass Chars. Energy Fuels 2018;32:10695–700. https://doi.org/10.1021/acs.energyfuels.8b02288.
[20] Lam PS, Sokhansanj S, Bi X, Lim CJ, Melin S. Energy Input and Quality of Pellets Made from Steam-Exploded Douglas Fir (Pseudotsuga menziesii). Energy Fuels 2011;25:1521–8. https://doi.org/10.1021/ef101683s.
[21] Legarra M, Morgan T, Turn S, Wang L, Skreiberg Ø, Antal MJ. Effect of Processing Conditions on the Constant-Volume Carbonization of Biomass. Energy Fuels 2019;33:2219–35. https://doi.org/10.1021/acs.energyfuels.8b03433.
[22] Legarra M, Morgan T, Turn S, Wang L, Skreiberg Ø, Antal MJ. Carbonization of Biomass in Constant-Volume Reactors. Energy Fuels 2018;32:475–89. https://doi.org/10.1021/acs.energyfuels.7b02982.
[23] Li K, Khanna R, Zhang J, Liu Z, Sahajwalla V, Yang T, et al. The evolution of structural order, microstructure and mineral matter of metallurgical coke in a blast furnace: A review. Fuel 2014;133:194–215. https://doi.org/10.1016/j.fuel.2014.05.014.
[24] Lindstad T, Syvertsen M, Ishak R, Arntzen H. THE INFLUENCE OF ALKALIS ON THE BOUDOUARD REACTION. 2004.
[25] Lu Z, Jian J, Jensen PA, Wu H, Glarborg P. Influence of Torrefaction on Single Particle Combustion of Wood. Energy Fuels 2016;30:5772–8. https://doi.org/10.1021/acs.energyfuels.6b00806.
[26] Manyà JJ, Alvira D, Azuara M, Bernin D, Hedin N. Effects of Pressure and the Addition of a Rejected Material from Municipal Waste Composting on the Pyrolysis of Two-Phase Olive Mill Waste. Energy Fuels 2016;30:8055–64. https://doi.org/10.1021/acs.energyfuels.6b01579.
[27] Manyà JJ, Ortigosa MA, Laguarta S, Manso JA. Experimental study on the effect of pyrolysis pressure, peak temperature, and particle size on the potential stability of vine shoots-derived biochar. Fuel 2014;133:163–72. https://doi.org/10.1016/j.fuel.2014.05.019.

[28] Phounglamcheik A, Vila R, Kienzl N, Wang L, Hedayati A, Broström M, et al. CO2Gasification Reactivity of Char from High-Ash Biomass. ACS Omega 2021;6:34115–28. https://doi.org/10.1021/acsomega.1c05728.
[29] Phounglamcheik A, Wang L, Romar H, Kienzl N, Broström M, Ramser K, et al. Effects of Pyrolysis Conditions and Feedstocks on the Properties and Gasification Reactivity of Charcoal from Woodchips. Energy Fuels 2020;34:8353–65. https://doi.org/10.1021/acs.energyfuels.0c00592.
[30] Phounglamcheik A, Wretborn T, Umeki K. Increasing Efficiency of Charcoal Production with Bio-Oil Recycling. Energy Fuels 2018;32:9650–8. https://doi.org/10.1021/acs.energyfuels.8b02333.
[31] Pusz S, Krzesińska M, Smędowski Ł, Majewska J, Pilawa B, Kwiecińska B. Changes in a coke structure due to reaction with carbon dioxide. Int J Coal Geol 2010;81:287–92. https://doi.org/10.1016/j.coal.2009.07.013.
[32] Riva L, Nielsen HK, Skreiberg Ø, Wang L, Bartocci P, Barbanera M, et al. Analysis of optimal temperature, pressure and binder quantity for the production of biocarbon pellet to be used as a substitute for coke. Appl Energy 2019:256. https://doi.org/10.1016/j.apenergy.2019.113933.
[33] Riva L, Wang L, Ravenni G, Bartocci P, Buø TV, Skreiberg Ø, et al. Considerations on factors affecting biochar densification behavior based on a multiparameter model. Energy 2021:221. https://doi.org/10.1016/j.energy.2021.119893.
[34] Rorvik S, Lossius LP. Characterization of Prebake Anodes by Micro X-ray Computed Tomography 2017. https://doi.org/10.1007/978-3-319-51541-0_148.
[35] Schneider C, Rincón Prat S, Kolb T. Determination of active sites during gasification of biomass char with CO2 using temperature-programmed desorption. Part 1: Methodology & desorption spectra. Fuel 2020;267:116726. https://doi.org/10.1016/j.fuel.2019.116726.
[36] Schneider C, Walker S, Phounglamcheik A, Umeki K, Kolb T. Effect of calcium dispersion and graphitization during high-temperature pyrolysis of beech wood char on the gasification rate with CO2. Fuel 2021;283:118826. https://doi.org/10.1016/j.fuel.2020.118826.
[37] Schneider CA, Rasband WS, Eliceiri KW. NIH Image to ImageJ: 25 years of image analysis. Nat Methods 2012;9:671–5. https://doi.org/10.1038/nmeth.2089.
[38] Skreiberg Ø, Wang L, Bach Q-V, Grønli M. Carbonization pressure influence on fixed carbon yield. Chem Eng Trans 2018;65:7–12. https://doi.org/10.3303/CET1865002.
[39] Sommerfeld M, Friedrich B. Replacing fossil carbon in the production of ferroalloys with a focus on bio-based carbon: A review. Minerals 2021:11. https://doi.org/10.3390/min11111286.
[40] Strandberg A, Holmgren P, Wagner DR, Molinder R, Wiinikka H, Umeki K, et al. Effects of Pyrolysis Conditions and Ash Formation on Gasification Rates of Biomass Char. Energy Fuels 2017;31:6507–14. https://doi.org/10.1021/acs.energyfuels.7b00688.
[41] Suopajärvi H, Umeki K, Mousa E, Hedayati A, Romar H, Kemppainen A, et al. Use of biomass in integrated steelmaking – Status quo, future needs and comparison to other low-CO2 steel production technologies. Appl Energy 2018;213:384–407. https://doi.org/10.1016/j.apenergy.2018.01.060.
[42] Surup GR, Trubetskaya A, Tangstad M. Charcoal as an Alternative Reductant in Ferroalloy Production: A Review. Processes 2020;8:1432. https://doi.org/10.3390/pr8111432.
[43] Ueki Y, Nunome Y, Yoshiie R, Naruse I, Nishibata Y, Aizawa S. Effect of Woody Biomass Addition on Coke Properties. ISIJ Int 2014;54:2454–60. https://doi.org/10.2355/isijinternational.54.2454.
[44] Van Wesenbeeck S, Wang L, Ronsse F, Prins W, Skreiberg O, Antal MJ. Charcoal "mines" in the Norwegian Woods. Energy Fuels 2016;30:7959–70. https://doi.org/10.1021/acs.energyfuels.6b00919.
[45] Sam VW, Wang L, Ronsse F, Prins W, Skreiberg Ø, Antal Jr. MJ. Charcoal "Mines" in the Norwegian Woods. Energy Fuels 2016;30:7959–70. https://doi.org/10.1021/acs.energyfuels.6b00919.
[46] Videgain M, Manyà JJ, Vidal M, Correa EC, Diezma B, García-Ramos FJ. Influence of feedstock and final pyrolysis temperature on breaking strength and dust production of wood-derived biochars. Sustain Switz 2021:13. https://doi.org/10.3390/su132111871.
[47] Wang L, Hovd B, Bui H-H, Valderhaug A, Buø TV, Birkeland RG, et al. CO2 reactivity assessment of woody biomass biocarbons for metallurgical purposes. Chem Eng Trans 2016;50:55–60. https://doi.org/10.3303/CET1650010.
[48] Wang L, Riva L, Skreiberg Ø, Khalil R, Bartocci P, Yang Q, et al. Effect of torrefaction on properties of pellets produced from woody biomass. Energy Fuels 2020;34:15343–54. https://doi.org/10.1021/acs.energyfuels.0c02671.
[49] Wang L, Skreiberg Ø, Smith-Hanssen N, Jayakumari S, Jahrsengene G, Rørvik S, et al. Investigation of the Properties and Reactivity of Biocarbons at High Temperature in a Mixture of CO/CO2. Chem Eng Trans 2022;92:697–702. https://doi.org/10.3303/CET2292117.
[50] Wang L, Skreiberg O, Van Wesenbeeck S, Grønli M, Antal MJ. Experimental Study on Charcoal Production from Woody Biomass. Energy Fuels 2016;30:7994–8008. https://doi.org/10.1021/acs.energyfuels.6b01039.
[51] Wang L, Várhegyi G, Skreiberg Ø, Li T, Grønli M, Antal Jr MJ. Combustion Characteristics of Biomass Charcoals Produced at Different Carbonization Conditions: A Kinetic Study. Energy Fuels 2016;30:3186–97. https://doi.org/10.1021/acs.energyfuels.6b00354.
[52] Liang W, Lukas B, Oyvind S, Goril J, Stein R. Effect of Calcination Temperature and Time on Properties of Steam Exploded Pellets. Chem Eng Trans 2022;92:355–60. https://doi.org/10.3303/CET2292060.
[53] Xie Y, Wang L, Li H, Westholm LJ, Carvalho L, Thorin E, et al. A critical review on production, modification and utilization of biochar. J Anal Appl Pyrolysis 2022;161:105405. https://doi.org/10.1016/j.jaap.2021.105405.
[54] Ye L, Peng Z, Wang L, Anzulevich A, Bychkov I, Kalganov D, et al. Use of Biochar for Sustainable Ferrous Metallurgy. JOM 2019;71:3931–40. https://doi.org/10.1007/s11837-019-03766-4.
[55] Yu Y, Wu J, Ren X, Lau A, Rezaei H, Takada M, et al. Steam explosion of lignocellulosic biomass for multiple advanced bioenergy processes: A review. Renew Sustain Energy Rev 2022;154:111871. https://doi.org/10.1016/j.rser.2021.111871.
[56] Zhang H. Relationship of Coke Reactivity and Critical Coke Properties. Metall Mater Trans B 2019;50:204–9. https://doi.org/10.1007/s11663-018-1438-x.